

Effects of attenuation, velocity and density on SH-wave reflection/transmission coefficients in isotropic, weakly attenuating media

Miłosz Wcisło^{1,2}

¹Institute of Rock Structure and Mechanics, Acad. Sci. of CR, V Holešovičkách 41m, 182 09, Praha 8, Czech Republic

²Faculty of Mathematics and Physics, Charles University, V Holešovičkách 747/2, 180 00, Praha 8, Czech Republic.

E-mail: wcislo@irsm.cas.cz

Summary

Study of the SH-wave reflection and transmission coefficients in attenuative media using perturbation approach (Weak Attenuation Concept - WAC) is conducted. It shows that differences in respect to the elastic reference have greatest magnitude for angles close to the critical incidence in the reference elastic medium. In this region, value of the modulus of the coefficient is reduced. For majority of models, these regions cannot be studied with the use of WAC only inside narrow interval close the critical angle (± 2 degrees), where the results are influenced by singularity of the WAC formulas. Smaller deviations are encountered in the vicinity of the Brewster angle, where in anelastic case reflection coefficient is not equal to zero. Effects of changes of attenuation, density and velocity of the medium on calculated coefficients are studied. Tests indicate that contrast in quality factors between layers contributes most to the differences in respect to elastic reference. Furthermore, changes in velocity have particularly interesting results. With higher contrast in velocities between layers, the difference at the Brewster angle is increasing, but in the vicinity of critical angle is decreasing. Investigation of effects of inhomogeneity of the slowness vector of the incident wave and tests of accuracy of the approximation are included in the study.

1. Introduction

Pšenčík & Wcisło (2018) provide simple expressions for reflection and transmission (R/T) coefficients that are based on the perturbation approach and as demonstrated, work even for relatively high attenuation. In this study we concentrate on testing the anelastic reflection and transmission coefficients using various models with different values of Q factor, density and velocity. Previous studies (eg. Daley & Krebes, 2015, Ursin et al., 2017) have shown that the anelasticity results in the biggest differences in respect to elastic reference in the vicinity of the critical angle. Formulas of Pšenčík & Wcisło fail in the vicinity of the critical angle; nevertheless we will show that the error caused by the existing singularity is not significant outside of the interval ± 2 deg from the critical angle for majority of models. This

realization allows us to focus on broader region close to the critical angle where the effect of the attenuation is still significant and the approximation works reasonably well. Another object of interest is Brewster angle where the effect of anelasticity is noticeable as well.

2. SH- Reflection and transmission coefficients in Weak Attenuation Concept

To test the influence of different values of density, velocity, attenuation and their contrasts between layers we will use perturbation approach presented by Pšenčík and Wcisło (2018). For reflection coefficient the formulae has a form:

$$R = \frac{\rho_1 \beta_1^2 (1 - iQ_1^{-1})(P_i + iA_i)N_i - \rho_2 \beta_2^2 (1 - iQ_2^{-1})(P_i^{(t)} + iA_i^{(t)})N_i}{\rho_1 \beta_1^2 (1 - iQ_1^{-1})(P_i + iA_i)N_i + \rho_2 \beta_2^2 (1 - iQ_2^{-1})(P_i^{(t)} + iA_i^{(t)})N_i} \quad [1]$$

and analogously for transmission coefficient:

$$T = \frac{2\rho_1 \beta_1^2 (1 - iQ_1^{-1})(P_i + iA_i)N_i}{\rho_1 \beta_1^2 (1 - iQ_1^{-1})(P_i + iA_i)N_i + \rho_2 \beta_2^2 (1 - iQ_2^{-1})(P_i^{(t)} + iA_i^{(t)})N_i} \quad [2]$$

where \mathbf{P} is propagation vector, \mathbf{A} is attenuation vector both of which are sub-vectors of the slowness vector. \mathbf{N} is unit vector normal to the interface. For the subcritical incidence, the slowness vector of the incident wave assumes a form:

$$p_i = P_i + iA_i = P_i + i\left(\frac{1}{2}Q_1^{-1}P_i + Dm_i\right) \quad [3]$$

where \mathbf{D} is the inhomogeneity factor and \mathbf{m}_i is an unit vector perpendicular to the propagation vector situated in the plane formed by \mathbf{N} and \mathbf{P} . Inhomogeneity of the slowness vector can be described as well using so called inhomogeneity angle γ . Example of inhomogeneous slowness vector is shown in Figure 1. In case the inhomogeneity factor (angle) is equal 0 (both propagation and attenuation vectors point in the same direction) the wave is called homogeneous.

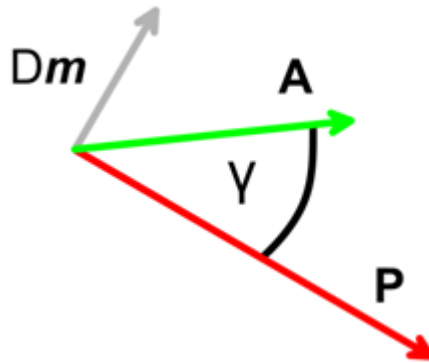


Fig. 1. Illustration of inhomogeneous slowness vector

Given that the slowness vector at the interface needs to satisfy relations resulting from the approximate complex valued eikonal equation and Snell's law for the complex valued slowness vector, propagation and attenuation vectors for transmitted wave are of more complicated form. For the subcritical incidence:

Propagation vector:

$$\begin{aligned}
 P_i^{(t)} &= P_i - N_i \beta_1^{-1} X_1 + N_i \beta_2^{-1} X_2 \\
 X_1 &= (1 - \beta_1^2 p^2)^{1/2} \\
 X_2 &= (1 - \beta_2^2 p^2)^{1/2}
 \end{aligned} \tag{4}$$

Attenuation vector:

$$\begin{aligned}
 A_i^{(t)} &= A_i - N_i \beta_1^{-1} \xi + N_i \beta_2^{-1} \xi^{(t)} \\
 \xi &= \frac{1}{2} Q_1^{-1} X_1 + \beta_1 D m_i N_i \\
 \xi^{(t)} &= \frac{1}{2} Z X_2^{-1} \\
 Z &= Q_2^{-1} - r^2 Q_1^{-1} + 2X_1 r^2 \xi \\
 r &= \beta_2 / \beta_1
 \end{aligned} \tag{5}$$

where, p is ray parameter. Propagation vector is of the first order while attenuation vector is of the second order. Quantity Z determines the orientation of the attenuation vector for the subcritical incidence. If Z is positive, the attenuation vector points to the medium the wave is propagating into, otherwise attenuation vector points back to the medium the wave is propagating from. It means that attenuation vector is not necessarily pointing towards the same medium as the propagation vector. For overcritical incidence, the propagation and attenuation vectors have following form:

Propagation vector:

$$\begin{aligned}
 P_i^{(t)} &= P_i - N_i \beta_1^{-1} X_1 + N_i \beta_2^{-1} \bar{\xi}^{(t)} \\
 X_1 &= (1 - \beta_1^2 p^2)^{1/2} \\
 \xi^{(t)} &= \frac{1}{2} Z \bar{X}_2^{-1} \\
 Z &= Q_2^{-1} - r^2 Q_1^{-1} + 2X_1 r^2 \xi
 \end{aligned} \tag{6}$$

Attenuation vector:

$$A_i^{(t)} = A_i - N_i \beta_1^{-1} \xi + N_i \beta_2^{-1} \bar{X}_2$$

$$X_2 = i \bar{X}_2 = i(\beta_1^2 p^2 - 1)^{1/2} \quad [7]$$

$$\xi = \frac{1}{2} Q_1^{-1} X_1 + \beta_1 D m_i N_i$$

$$r = \frac{\beta_2}{\beta_1}$$

In case of over critical incidence both propagation and attenuation vectors are of first order. It means that in the overcritical region the attenuation vector may be of similar magnitude as the propagation vector (unlike for the subcritical incidence). Quantity Z affects propagation vector and this vector for different angles of incidence may point to the first or second medium.

Majority of tests are performed using realistic values of Q factor which are within the lower range of Q 's that are found within Earth's crust (<100), but also within the range of applicability of weak attenuation concept (WAC) as determined by Gajewski & Pšenčík (1991) for applications within layers ($Q > 50$). $Q_{SH} < 50$ are mainly found for rocks consisting medium near to the surface. Unless stated otherwise, we will be working with homogeneous incident waves.

3. General tests

First tests that we perform include 3 models with general differences between properties of layers. The first layer is the same in each model and has $\beta_1 = 2.0$ km/s, $\rho_1 = 2.0$ g/cm³ and $Q_1 = 50$, Second layer in each case is characterized by higher seismic impedance and Q - as usually harder rocks are less attenuative (Helle et al. 2004; Barton 2007). The contrast between properties of layers is increasing for consecutive models. Second layers have following parameters: $\beta_2 = 2.5$ km/s, $\rho_2 = 2.25$ g/cm³, $Q_2 = 75$ in the first case; $\beta_2 = 3.0$ km/s, $\rho_2 = 2.5$ g/cm³, $Q_2 = 100$ in the second case and $\beta_2 = 3.5$ km/s, $\rho_2 = 2.75$ g/cm³, $Q_2 = 125$. Obtained values of R/T coefficients are compared with results for reference elastic medium. Figures 2, 3 and 4 show real and imaginary parts of the reflection coefficient along with representation of coefficient as modulus and phase. Figures 5, 6 and 7 show results for transmission coefficients.

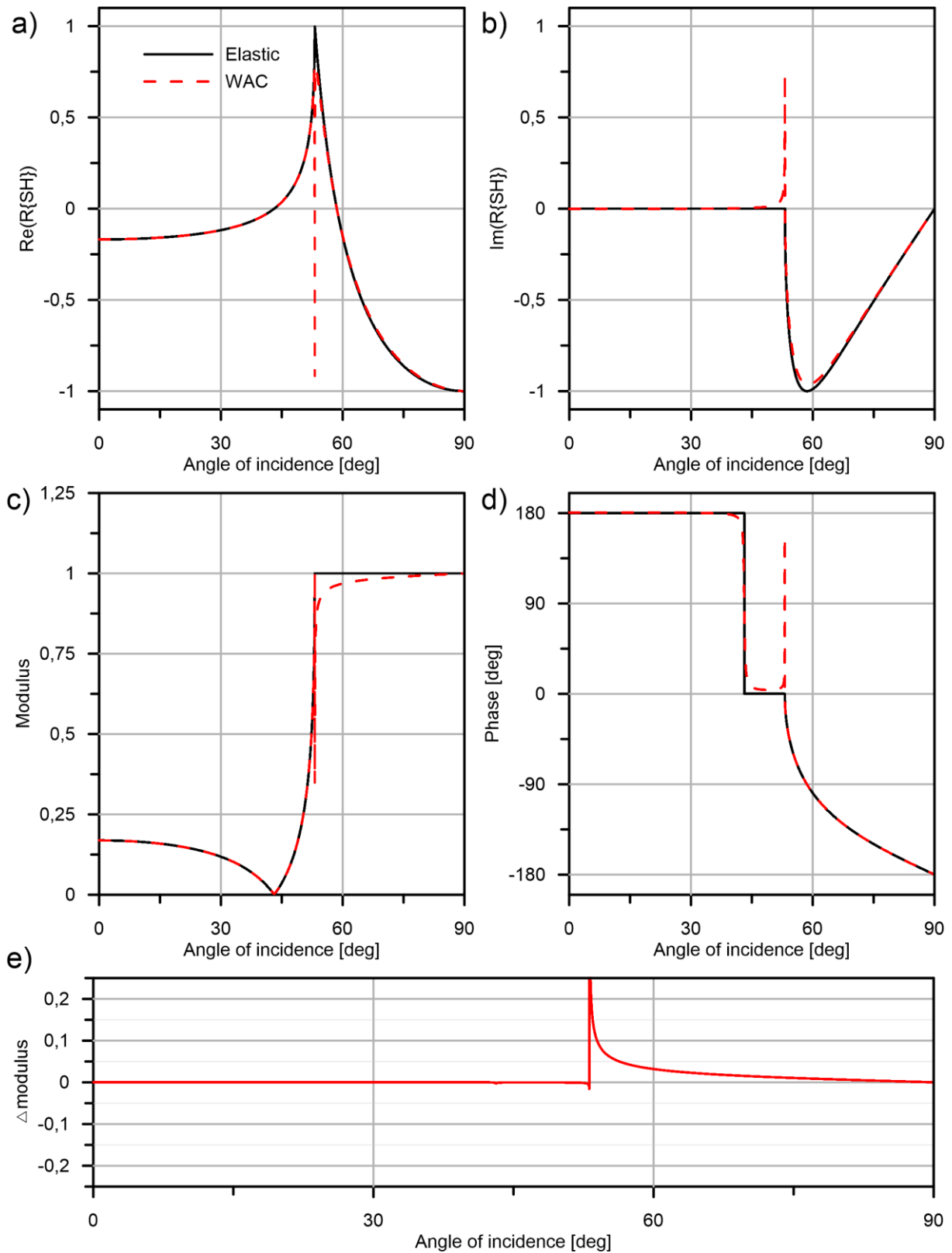


Fig. 2. a) Real parts of reflection coefficient calculated for model with $\beta_1=2.0$, $\rho_1=2.0$, $Q_1=50$ and $\beta_2=2.5$, $\rho_2=2.25$, $Q_2=75$ along with curve representing reference elastic model, b) imaginary parts of reflection coefficient, c) moduli of reflection coefficient, d) phases of reflection coefficient, e) difference between modulus of elastic reference model and modulus calculated using WAC.

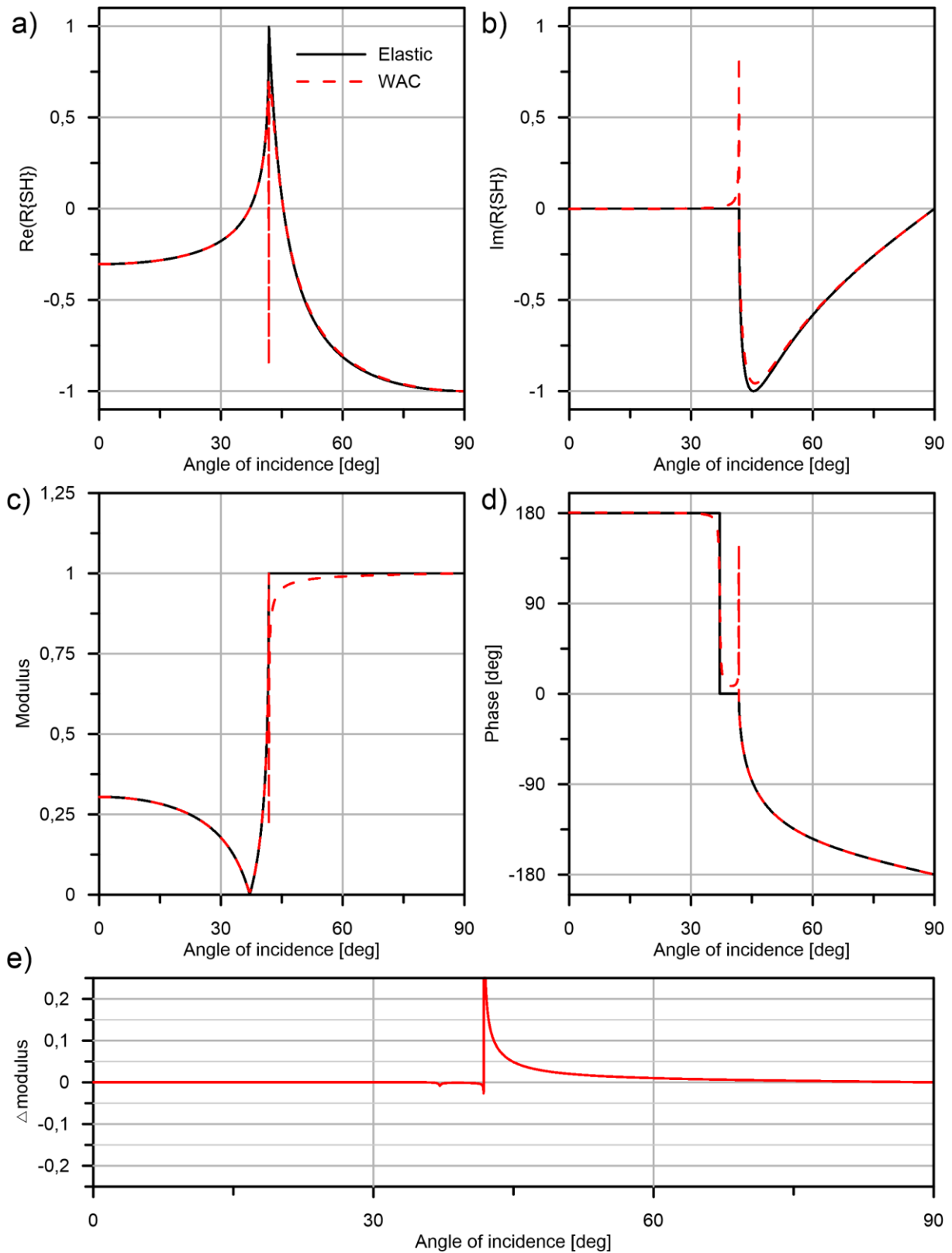


Fig. 3. a) Real parts of reflection coefficient calculated for model with $\beta_1=2.0$, $\rho_1=2.0$, $Q_1=50$, and $\beta_2=3.0$, $\rho_2=2.5$, $Q_2=100$ along with curve representing reference elastic model, b) imaginary parts of reflection coefficient, c) moduli of reflection coefficient, d) phases of reflection coefficient, e) difference between modulus of elastic reference model and modulus calculated using WAC.

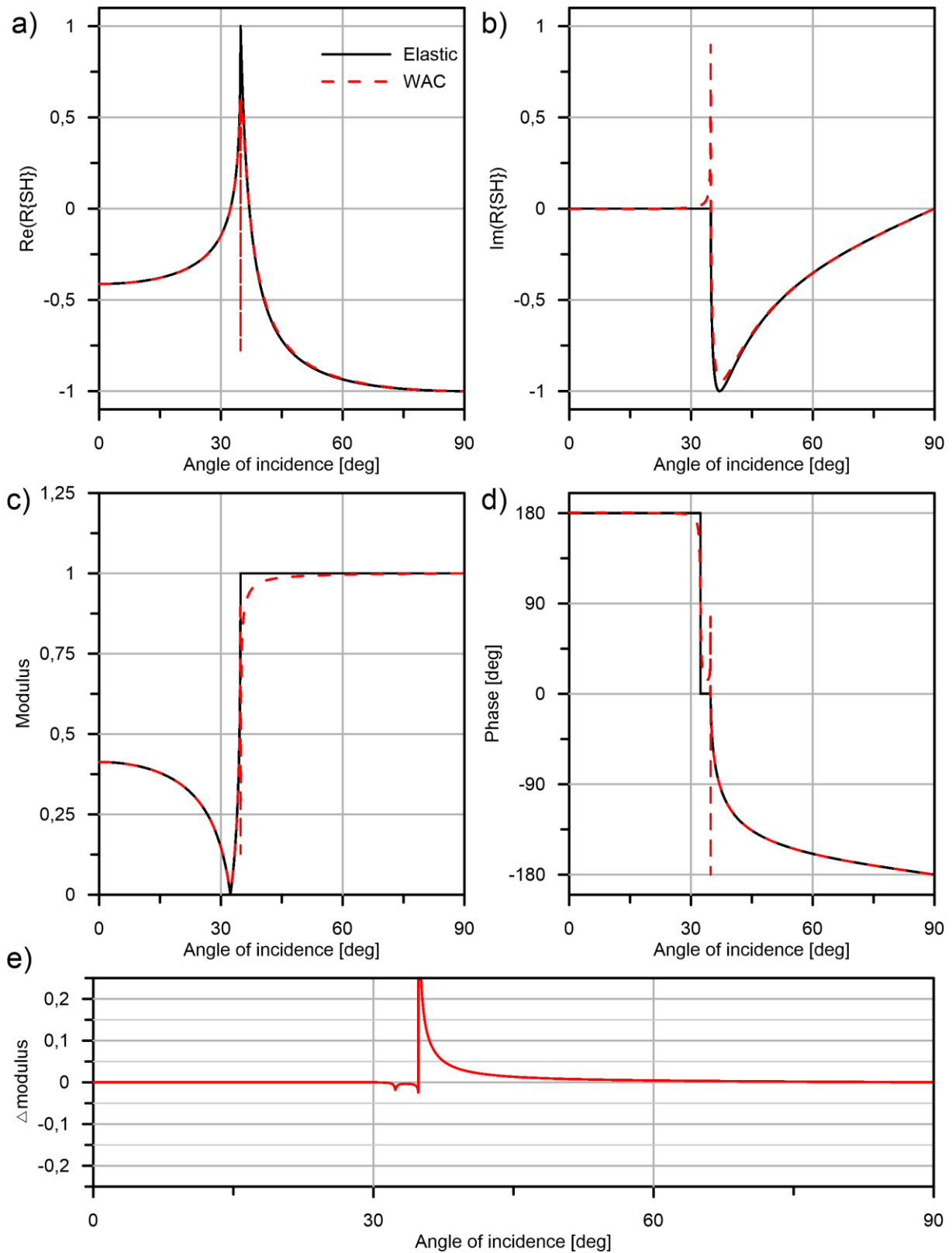


Fig. 4. a) Real parts of reflection coefficient calculated for model with $\beta_1=2.0$, $\rho_1=2.0$, $Q_1=50$, and $\beta_2=3.5$ $\rho_2=2.75$, $Q_2=125$ along with curve representing reference elastic model, b) imaginary parts of reflection coefficient, c) moduli of reflection coefficient, d) phase of reflection coefficient, e) difference between modulus of elastic reference model and modulus calculated using WAC.

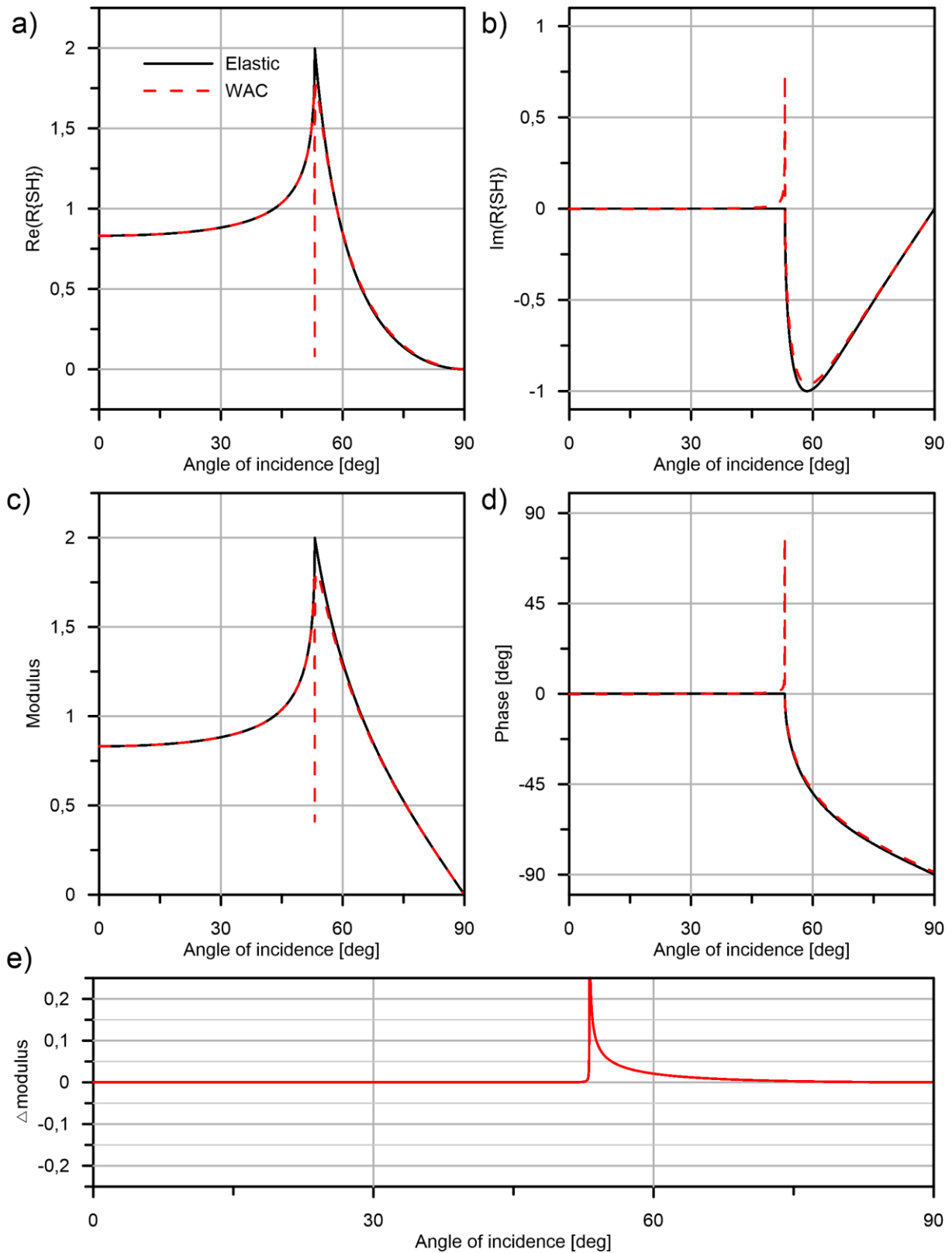


Fig. 5. a) Real parts of transmission coefficient calculated for model with $\beta_1=2.0$, $\rho_1=2.0$, $Q_1=50$, and $\beta_2=2.5$, $\rho_2=2.25$, $Q_2=75$ along with curve representing reference elastic model, b) imaginary parts of transmission coefficient, c) moduli of transmission coefficient, d) phases of transmission coefficient, e) difference between modulus of elastic reference model and modulus calculated using WAC.

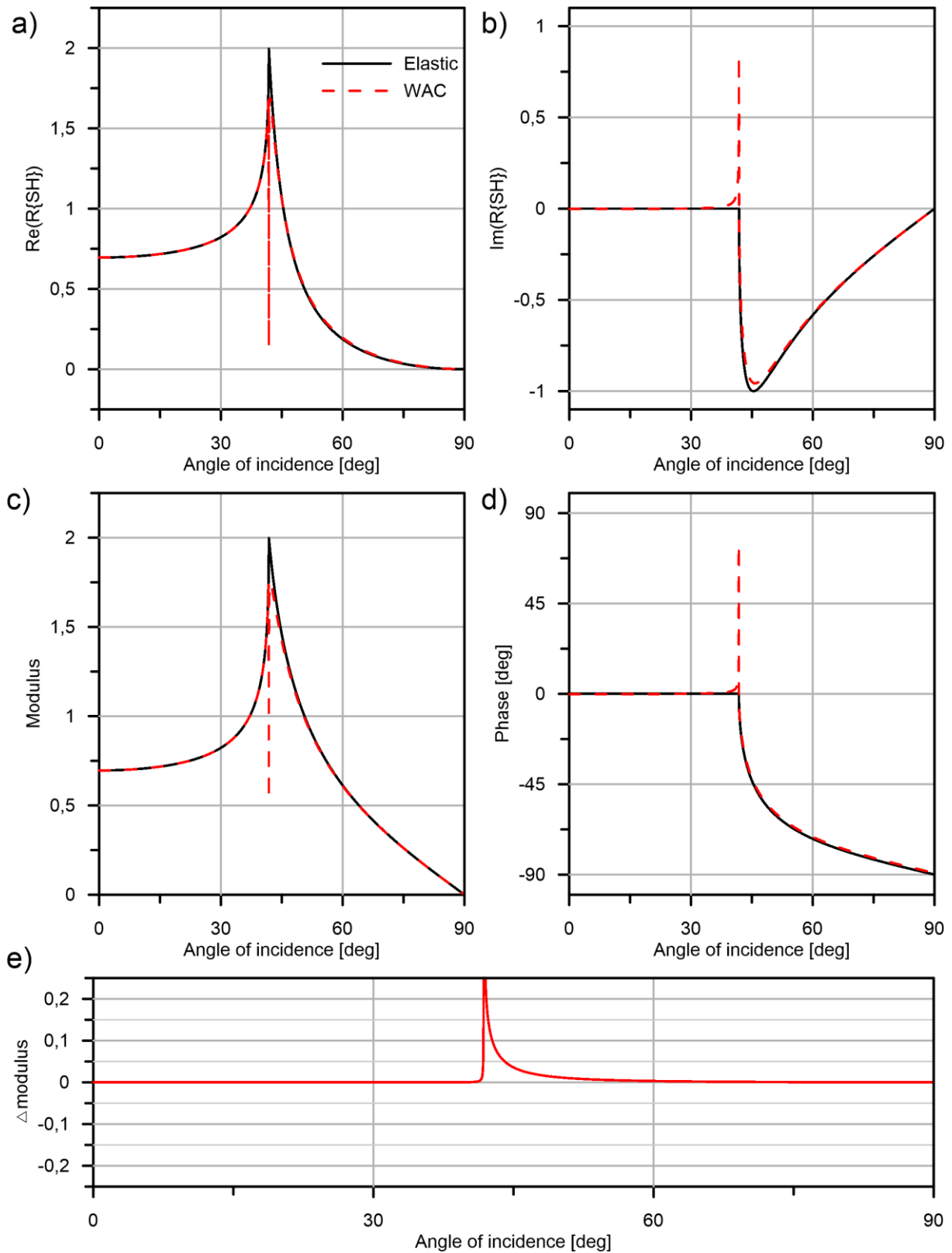


Fig. 6. a) Real part of transmission coefficients calculated for model with $\beta_1=2.0$, $\rho_1=2.0$, $Q_1=50$ and $\beta_2=3.0$, $\rho_2=2.5$, $Q_2=100$ along with curve representing reference elastic model, b) imaginary parts of transmission coefficient, c) moduli of transmission coefficient, d) phases of transmission coefficient, e) difference between modulus of elastic reference model and modulus calculated using WAC.

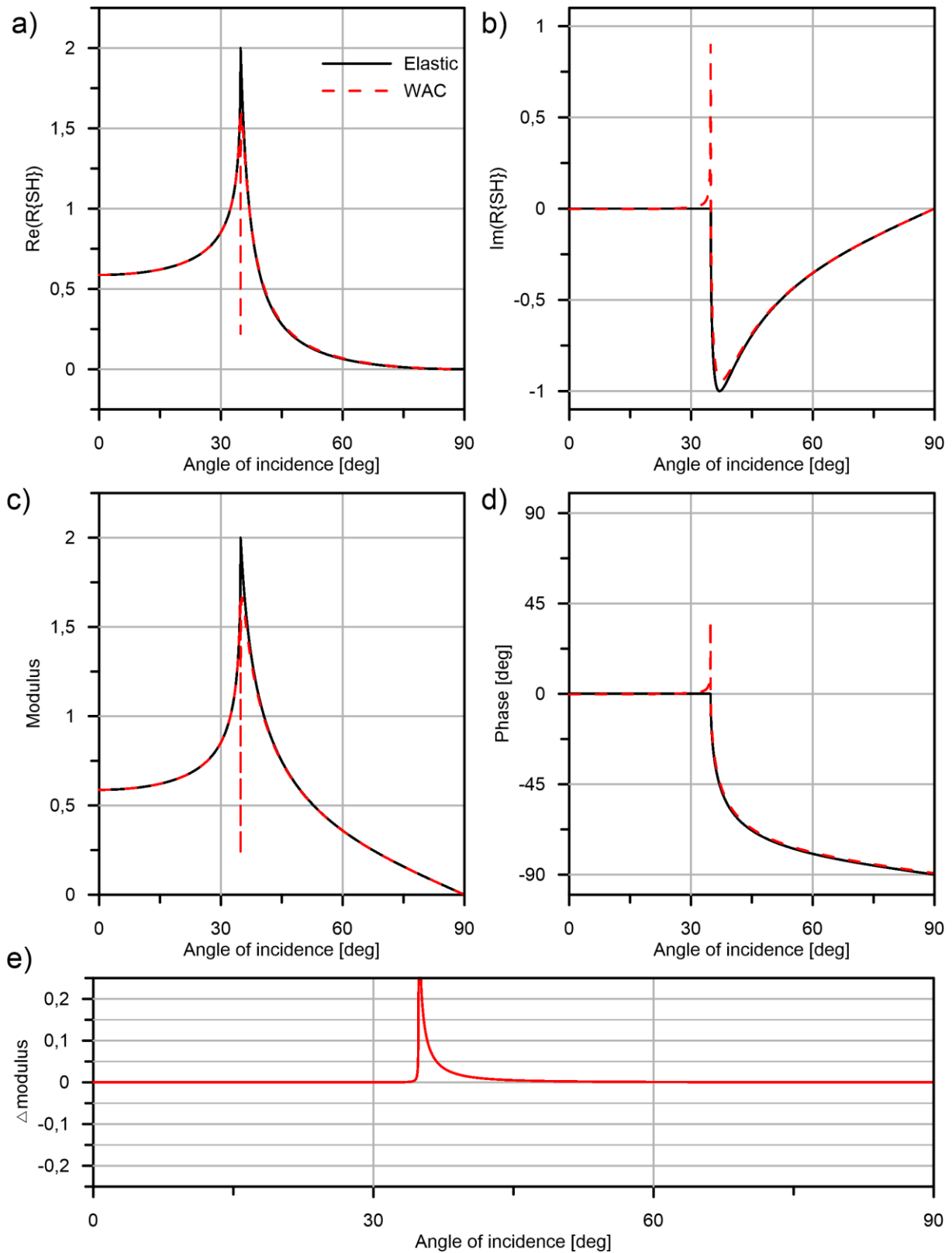


Fig. 7. a) Real parts of transmission coefficient calculated for model with $\beta_1=2.0$, $\rho_1=2.0$, $Q_1=50$ and $\beta_2=3.5$, $\rho_2=2.75$, $Q_2=125$ along with curve representing reference elastic model, b) imaginary parts of transmission coefficient, c) moduli of transmission coefficient, d) phases of transmission coefficient, e) difference between modulus of elastic reference model and modulus calculated using WAC.

We can note that the reflection coefficients calculated using WAC, are not particularly different in case of the subcritical incidence if we compare them to the elastic reference. The main difference is present in the vicinity of Brewster angle, where for the WAC coefficients the modulus is not equal to zero because of non-zero imaginary part. In the case of phase, at the Brewster angle, elastic coefficient implies discontinuity, with phase jumping from $+180$ degrees to 0 . In case of WAC the change is continuous, although still quick. The phase itself does not reach zero value. In the close vicinity of the critical angle, perturbation approach fails, although it should not be of high concern as the ray method does not work properly in this region as well. The difference between the WAC and elastic modulus is significantly higher for the overcritical incidence. Discarding values in close vicinity of the critical angle (± 2 degrees), which are affected by the singularity, the difference in respect to the elastic moduli may be above 0.1 further in this region. The difference for higher incident angles decreases and reflection coefficient calculated using WAC is close to elastic. For overcritical incidence the difference in calculated phases is small as both imaginary and real values are of the first order. The ratio of their magnitudes is not strongly affected by perturbation in this situation.

In case of transmission coefficients, the difference is visible only in the vicinity of the critical angle of the elastic reference as in case of transmission there is no region with behavior similar to vicinity of reflection's Brewster angle. The modulus of anelastic coefficient does not reach maximum value of two at the critical incidence as it does for elastic reference. The magnitude of difference is similar to one observed for reflection coefficient and analogously decreases as we move further away the critical incidence.

Figures 8 and 9 show differences between modulus of elastic and anelastic R/T coefficients for all three models. Figure 8 includes subcritical incidence and Figure 9 overcritical incidence. It allows us to better compare effect of attenuation for all three models. For model with highest contrast between layers, in case of subcritical incidence the difference between elastic and WAC modulus is the most pronounced. Model with smallest contrast results in lowest difference. In case of overcritical incidence this relationship is not straightforward. Initially for interval of $3-4$ degrees the difference is higher for model with greatest contrast. Further above the critical angle it is the model which has the smallest contrast that has the most pronounced difference. Nevertheless, we need to remember that the close vicinity of the critical incidence is influenced by the presence of the singularity of the WAC formulas. In order to check if the described behavior is just the artifact of the method, in the study there will be included a benchmark with independent method. Namely there will be shown a comparison with results of Brokešová and Červený (1998).

Calculation of R/T coefficients implies multiplication and division of quantities describing density, seismic velocity and seismic attenuation. Variations of each of those components have effect on calculated coefficient. Therefore, in further parts of the text we should investigate effect of isolated variations of each of those single parameters on the R/T coefficients calculated using perturbation approach. It shall help us in understanding when reflection and transmission coefficients differ most from the elastic reference.

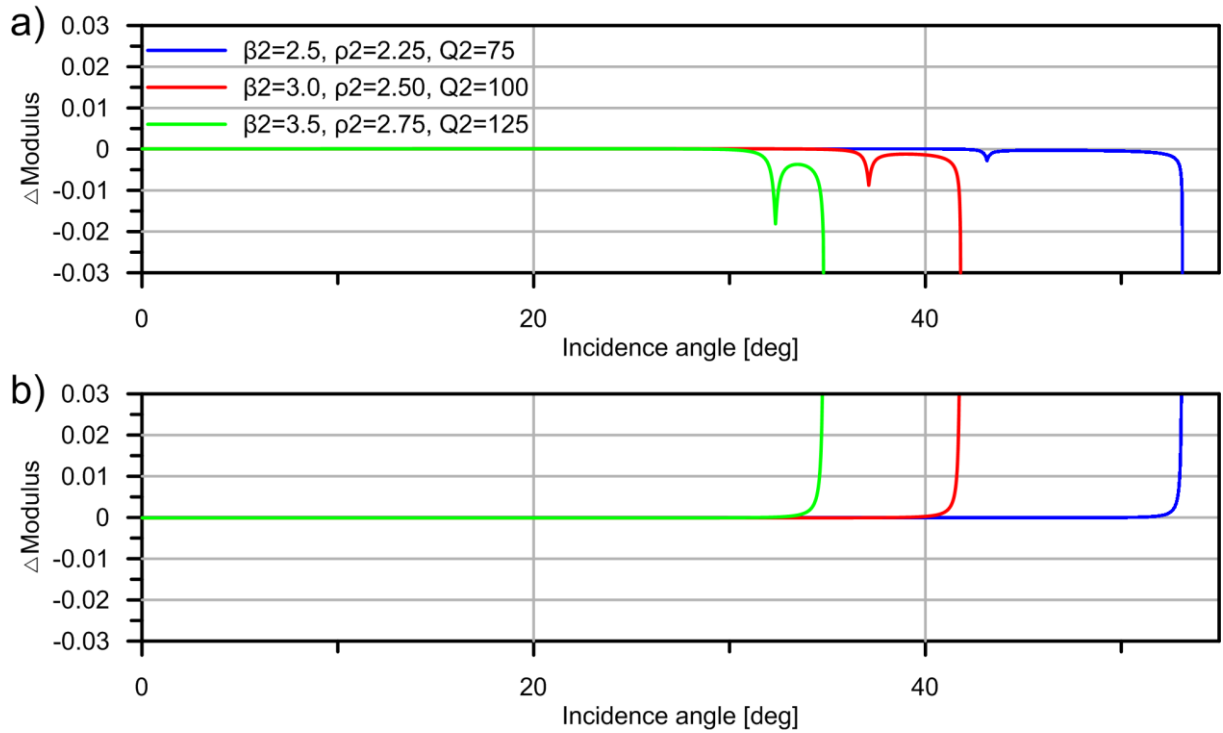


Fig. 8. a) the differences in the reflection coefficient for angles below the critical one, between the results for the elastic references and those obtained using WAC for models with $\beta_1=2.0$, $\rho_1=2.0$, $Q_1=50$ and different properties of the second layer, b) differences for transmission coefficient.

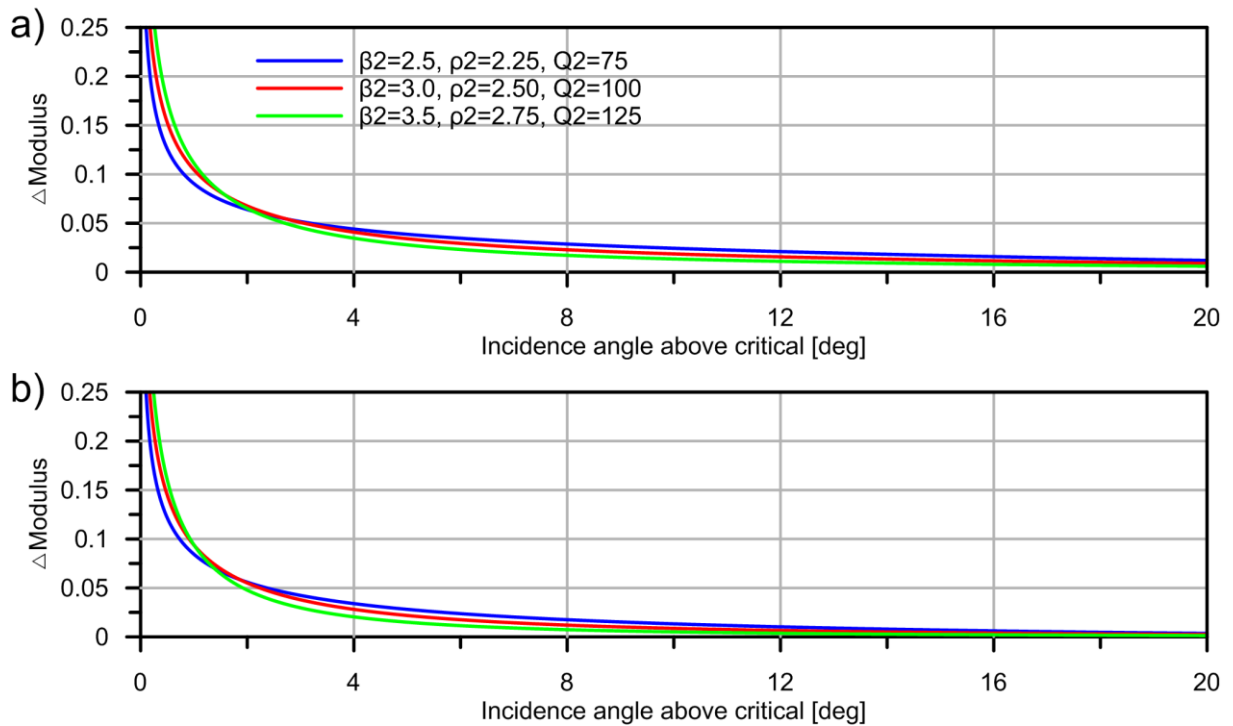


Fig. 9. a) the differences in the reflection coefficient for angles below the critical one, between the results for the elastic references and those obtained using WAC for models with $\beta_1=2.0$, $\rho_1=2.0$, $Q_1=50$ with different properties of the second layer, b) differences for transmission coefficient.

4. Reflection and Transmission coefficients for varying Q factor

As it is the attenuation that is causing the perturbation of the elastic reference case we may guess that it is the strength of the damping or its contrast between layers that shall have the crucial effect on difference between elastic reference and anelastic R/T coefficients. To investigate effects of changing Q we compute models with values of velocity and density being constant and the Q factor for the second layer changing. The first layer is characterized by $\beta_1=2.0$ km/s, $\rho_1=2.0$ g/cm³, $Q_1=50$, second layer is defined with $\beta_2=2.5$ km/s, $\rho_2=2.25$ g/cm³ which make the model corresponding to the one shown in Figures 2 and 5. The Q factor of the second layer changes and is equal 25, 50, 75, 100, 125 for 5 consecutive models. Real, imaginary parts of the coefficients as well as their modulus and phase for all 5 anelastic + reference elastic model are shown in Figure 10 (reflection) and 11 (transmission).

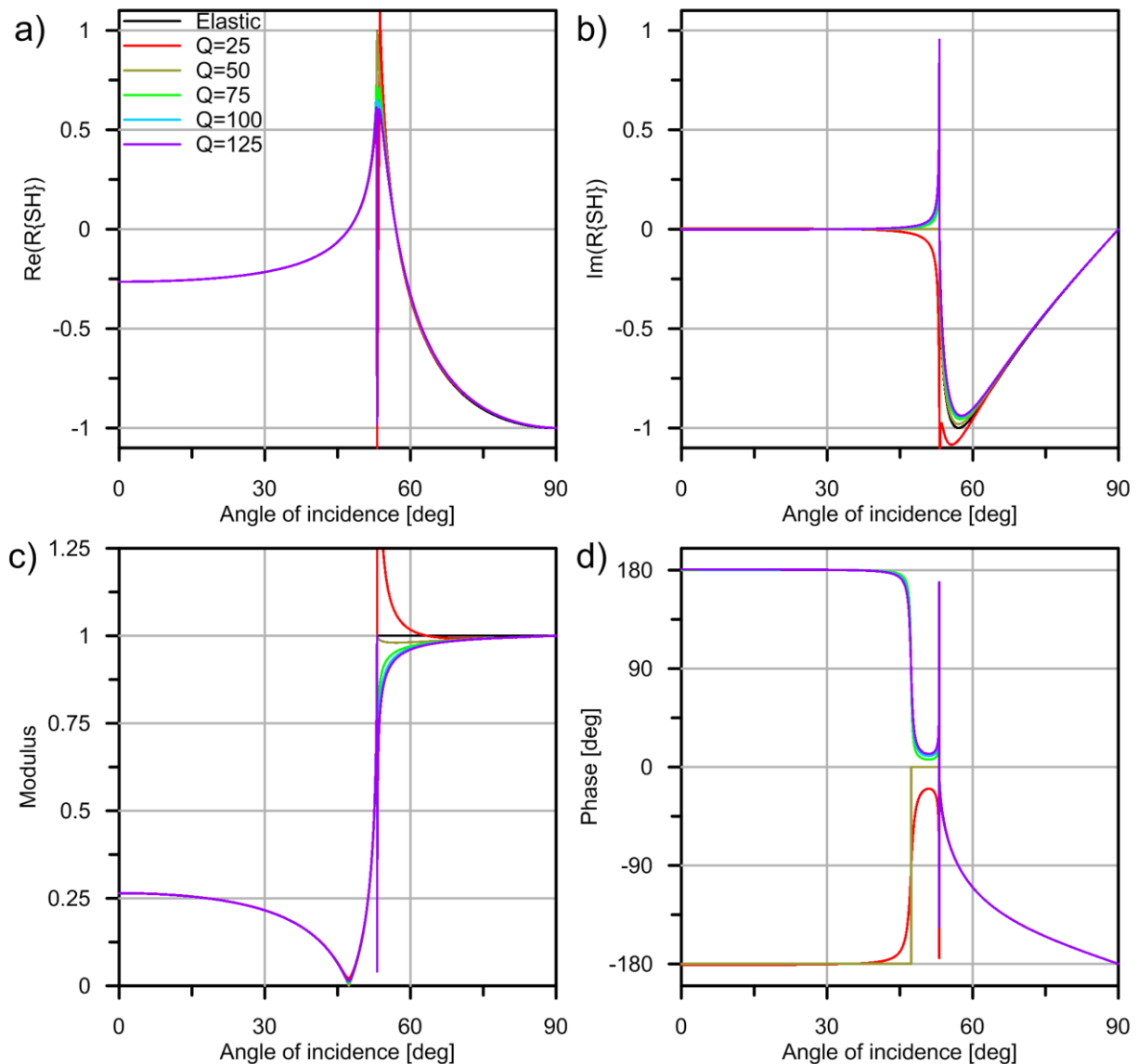


Fig. 10. a) real parts of the reflection coefficient for models with $\beta_1=2.0$ km/s, $\rho_1=2.0$ g/cm³, $Q_1=50$ and second layer characterized by $\beta_2=2.5$ km/s, $\rho_2=2.25$ g/cm³ and 5 different Q_2 values, along with the curve illustrating reference elastic model, b) imaginary parts of reflection coefficient, c) moduli of reflection coefficient, d) phases of reflection coefficient.

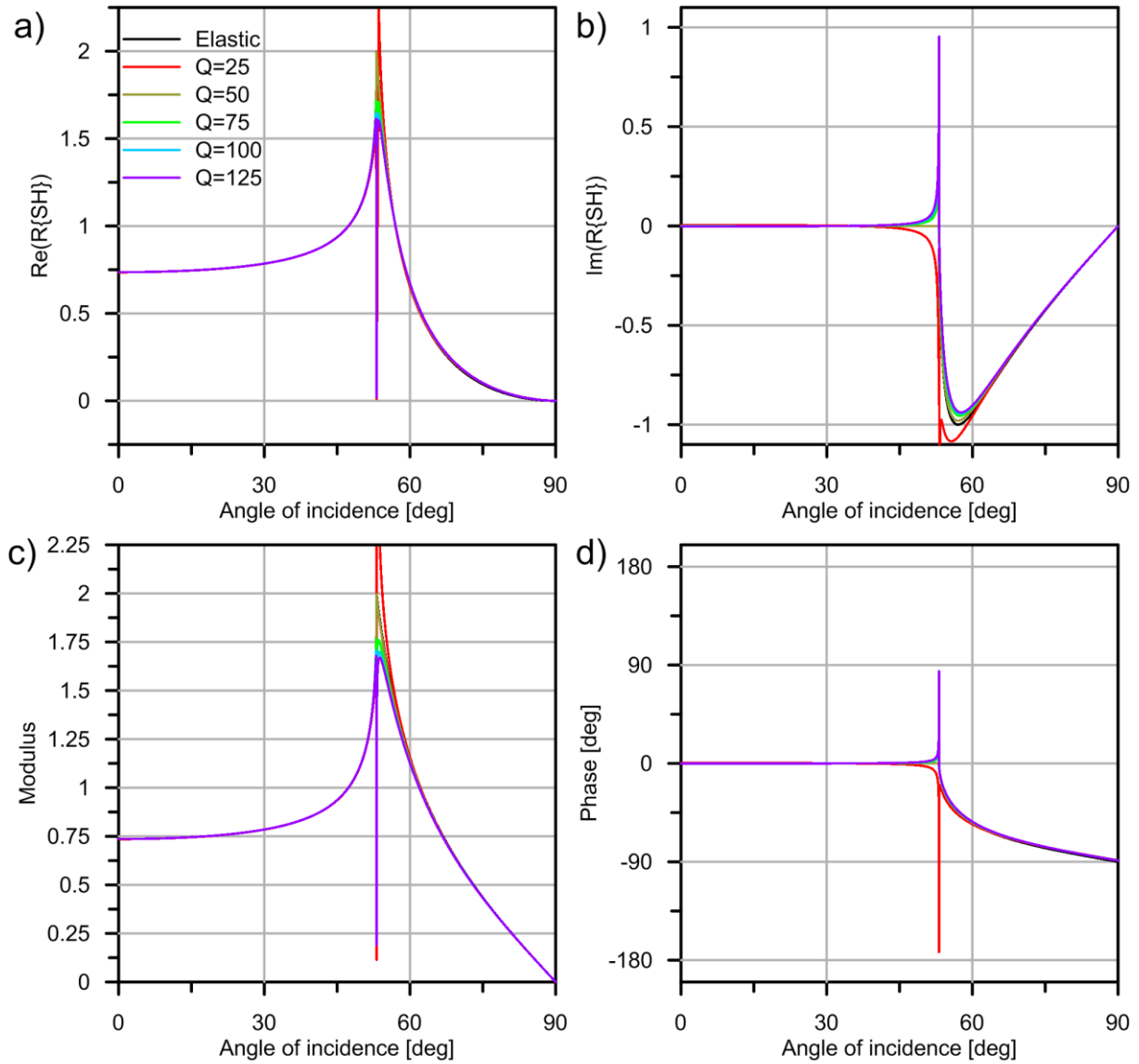


Fig. 11. a) real parts of the transmission coefficient for models with $\beta_1=2.0$ km/s, $\rho_1=2.0$ g/cm³, $Q_1=50$ and second layer characterized by $\beta_2=2.5$ km/s, $\rho_2=2.25$ g/cm³ and 5 different Q_2 values, along with the curve illustrating reference elastic model, b) imaginary parts of reflection coefficient, c) moduli of reflection coefficient, d) phases of reflection coefficient.

We can see that for both: reflection as well as transmission coefficient, the influence of changing Q is for most incident angles small and therefore the curves nearly overlay each other. The significant deviation between curves is present at the vicinity of the critical angle. If we are dealing with Q values that are higher for the second layer, as a result of the influence of the attenuation, the maximum of the real part of the coefficient is below 1 (reflection) or 2 (transmission) which are the maxima for the elastic reference (in case of presence of the critical angle). We can see that in the case of Q that is lower in the second layer the effect is opposite and implies increased maximum which leads to clearly incorrect results in the vicinity of the critical angle as the real value should not exceed stated size. Similar effect can be observed in case of imaginary part of the coefficient where for $Q_2=25$ the minimum is below -1 which is the extreme for the elastic reference. It is worth to note that it happens only when the velocity of the second layer is faster, yet the layer is more attenuative which is not likely to occur. Differences between elastic and anelastic case in big part depend on the contrast between strength of attenuation between layers. It is important to note that the contrast should be considered in relation to the values of $1/Q$ as it is the inverse Q value that

that we use in WAC formulas for the R/T coefficients and analogously we integrate along the ray to calculate the effect of the attenuation on the wave propagation (Aki & Richards, 2002). This is the reason why $Q_2=25$ ($Q_1^{-1}-Q_2^{-1}=0.02$) gives bigger discrepancy in respect to the elastic case than $Q_2=125$ ($Q_1^{-1}-Q_2^{-1}=0.012$).

To facilitate evaluation of the effect of attenuation and highlight differences between models, in Figures 12 and 13 we show the difference in values of modulus between the anelastic and elastic R/T coefficients. Figure 12 is showing values for subcritical incidence only, and Figure 13 is showing values for the overcritical incidence as the magnitude of differences varies for those two regions. In case of subcritical incidence the difference is present at the Brewster angle and increases with contrast between values of Q^{-1} . Further discrepancy is present close to the critical angle - in case of transmission coefficient it is the only range of the incidence where the discrepancy is somehow significant. Nevertheless we need to remember about presence of the singularity at the critical incidence for coefficients calculated using WAC. To illustrate how big interval does not provide accurate coefficients, in Figures 14 and 15 we show difference between the exact approach of Brokešová and Červený (1998) and results obtained using WAC. We can see that for the subcritical incidence in the vicinity of the critical angle, the differences between the elastic reference and WAC and differences between the exact approach of Brokešová and Červený and WAC are of similar magnitude. Therefore results for 2-3.5 degrees (bigger interval if contrast in Q^{-1} is high) below the critical angle should be discarded as caused by the error of the method. For overcritical incidence the difference is the strongest in the vicinity of the critical angle and further decreases. For overcritical incidence the interval with inaccuracy is relatively small (again ~ 2 degrees for models $Q_2 < Q_1$) comparing to the interval where differences between anelastic and elastic case are the most pronounced (~ 10 deg). Therefore, general trends shown in Figures 12 and 13 are correct although in the direct vicinity of the critical angle they are exaggerated if WAC is applied.

In case of overcritical incidence (for both, transmission and reflection) and example where the Q values are higher in the first layer while impedance in the first layer is smaller, results of the WAC are much worse and the curve converges to the proper values after ~ 25 degrees. The interval that is providing improper results is therefore very broad. Nevertheless, we should remember that in the presented case the difference in Q_2 values is very large. In further section of the paper we shall estimate range of angles where WAC cannot be applied in similar configuration for more realistic models.

The special case where both layers have the same Q values gives the same results as in the reference elastic case for subcritical incidence. This agrees with predictions of Buchen (1971). Still, for overcritical incidence the discrepancy is present (although not big) and it is caused by inaccuracy of the perturbation approach.

If we consider the R/T coefficient in respect to phases, the most interesting effects of anelasticity are visible between the vicinity of the Brewster angle and critical incidence. As previously noted for anelastic media Brewster Angle does not imply discontinuity for phase of reflection coefficient. The change becomes less sharp as we deal with stronger attenuation and with bigger contrast between layers. Further, the phase can approach zero from two sides. Either it approaches from the “negative” side and further stay negative until the critical reflection ($Q < 50$) or from the “positive” side and stay positive until critical angle ($Q > 50$).

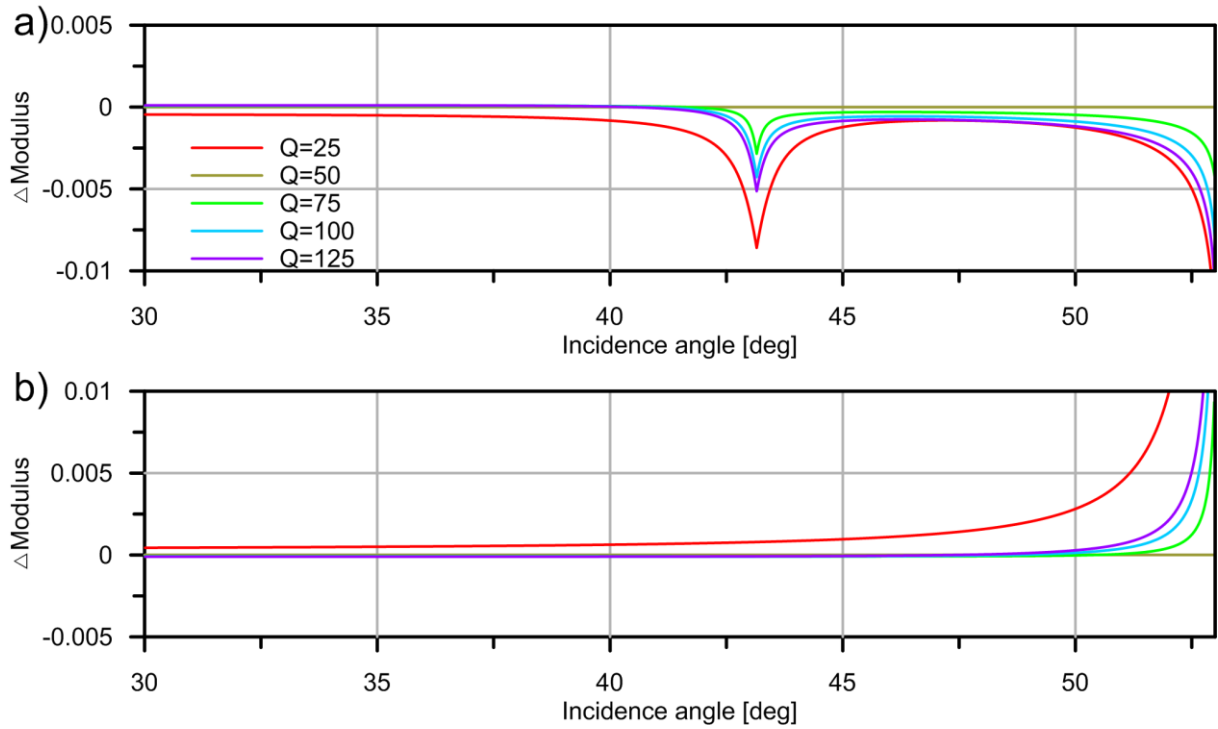


Fig. 12. a) differences between reference elastic reflection coefficient and coefficient calculated using WAC for models shown in Figure 10 – subcritical incidence, b) difference for transmission coefficient.

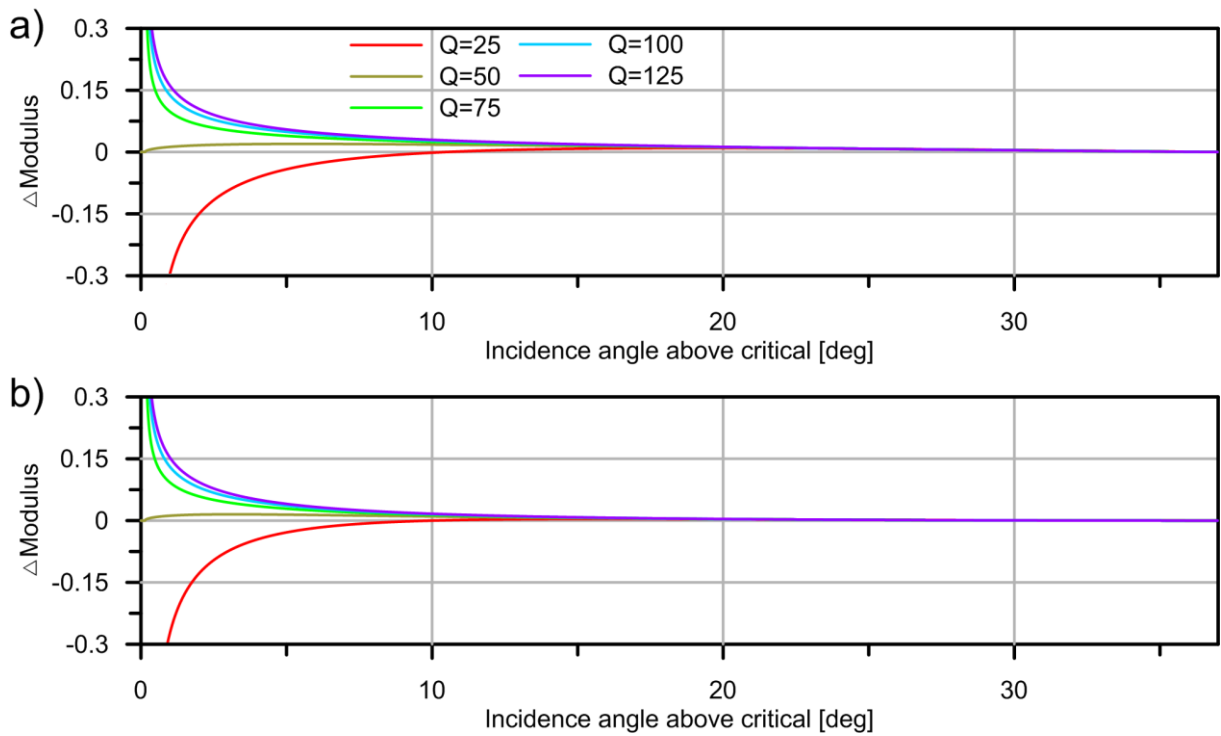


Fig. 13. a) differences between reference elastic reflection coefficient and coefficient calculated using WAC for models shown in Figure 10 – overcritical incidence, b) difference for transmission coefficient.

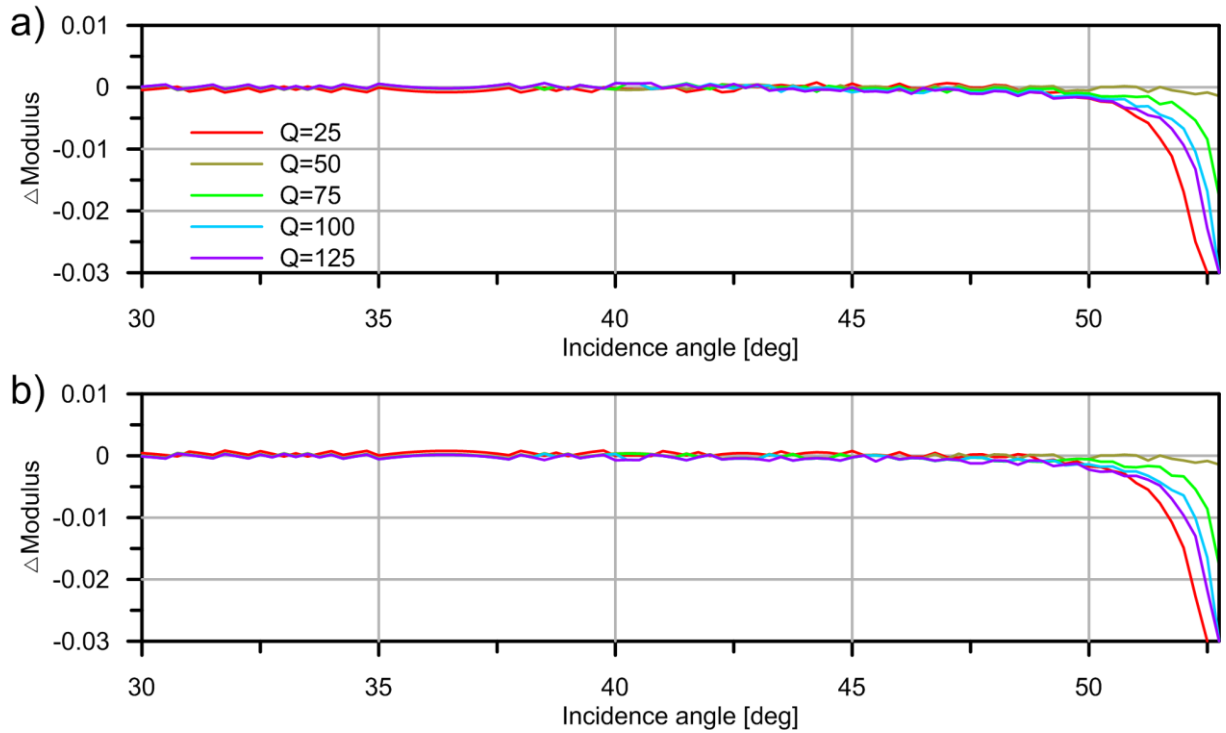


Fig. 14. a) differences between anelastic reflection coefficient calculated with exact approach of Brokešová and Červený (1998) and coefficient calculated using WAC for models shown in Figure 10 – subcritical incidence, reverberations of the curve are caused by different accuracy of computations for both methods, b) difference for transmission coefficient.

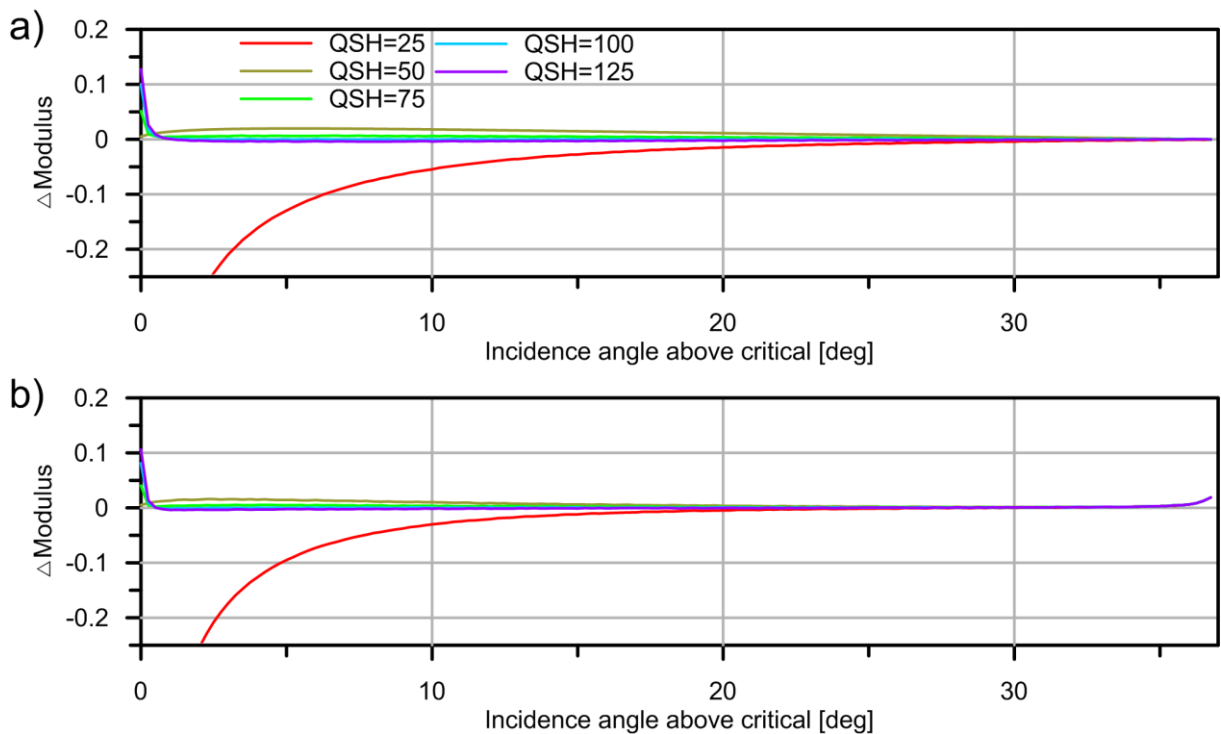


Fig. 15. a) differences between anelastic reflection coefficient calculated with exact approach of Brokešová and Červený (1998) and coefficient calculated using WAC for models shown in Figure 10 – overcritical incidence, b) difference for transmission coefficient.

5. Reflection and Transmission coefficients for varying densities

In this part of the study we shall investigate effects of varying density on the R/T coefficients calculated using WAC. We work with properties of the first layer being the same as in the previous part ($\beta_1=2.0$ km/s, $\rho_1=2.0$ g/cm³, $Q_1=50$). The second layer is characterized by $\beta_2=2.5$ km/s, $Q_2=75$ and varying values of ρ_2 assuming 1.75, 2.00, 2.25, 2.50 and 2.75 g/cm³ respectively. Real, imaginary parts of the coefficients as well as its modulus and phase for all 5 anelastic models are shown in Figure 16 (reflection) and 17 (transmission). We do not include in Figures curves showing reference elastic coefficients as they are different in each case and it would affect clarity of the graphs. Studied models have different values of imaginary and real part of elastic reference, therefore the interpretation of curves is not straightforward for this type of representation of coefficient's values. Although, we can note that e.g. for both, reflection and transmission coefficients, maxima of real values depend on the difference in the density between first and the second layer. For elastic reference models

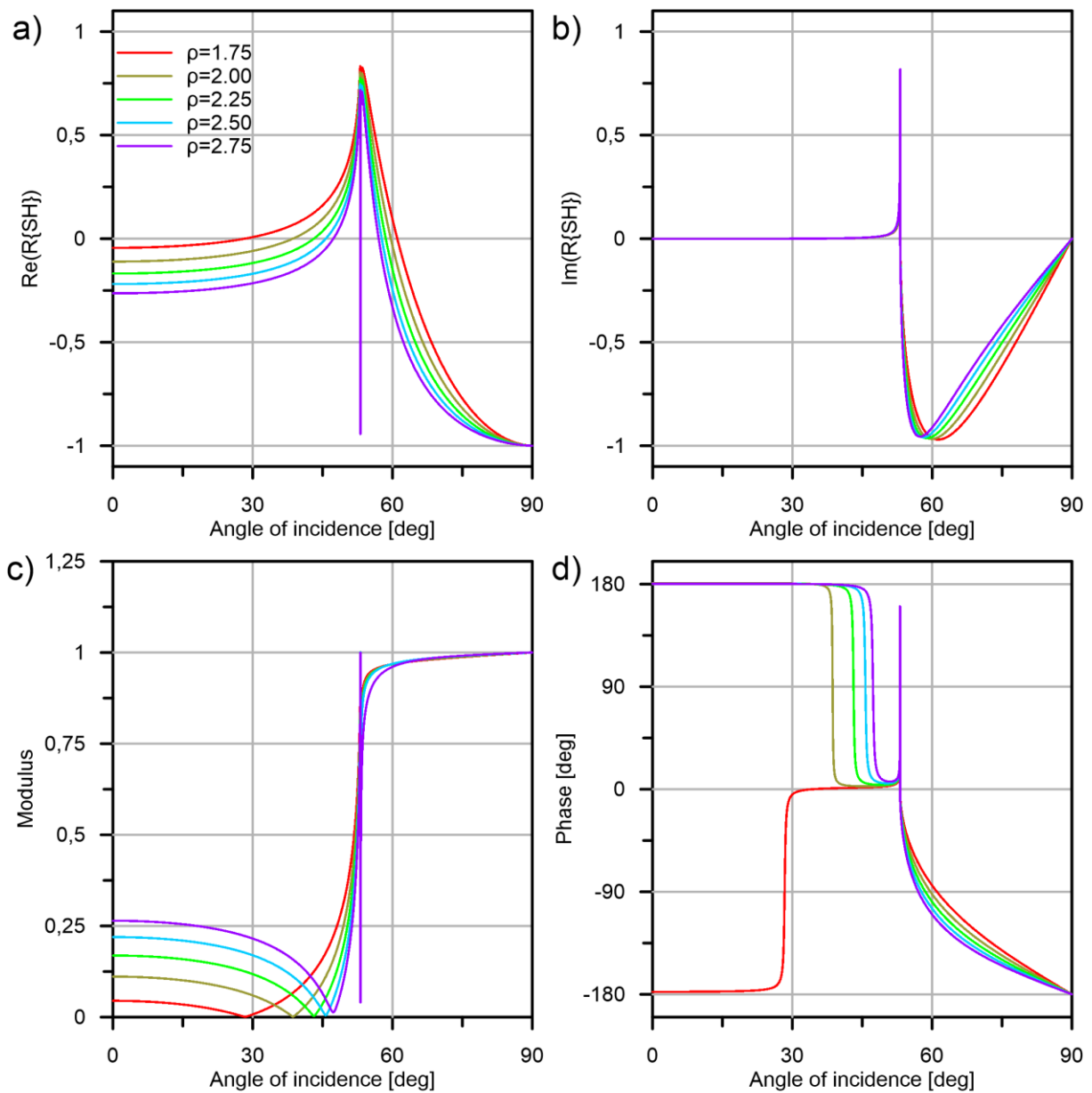


Fig. 16. a) real parts of the reflection coefficient for models with $\beta_1=2.0$ km/s, $\rho_1=2.0$ g/cm³, $Q_1=50$ and second layer characterized by $\beta_2=2.5$ km/s, $Q_2=75$ and 5 different ρ_2 values, b) imaginary parts of reflection coefficient, c) moduli of reflection coefficient, d) phases of reflection coefficient.

they are the same (1-reflection, 2-transmission). For both reflection and transmission, maximum of the real parts of the coefficient grow if the density of the second layer decreases and get smaller if the density of the second layer gets higher. To be able to properly see the effect of anelasticity we need to compare calculated coefficients with elastic reference. Figure 18 shows differences in modulus between elastic and anelastic coefficients for subcritical incidence. Figure 19 analogously illustrates differences for the overcritical incidence. We need to remember that the approximation fails in the vicinity of the critical angle, but it is worth to note that note, that the errors do not depend on the density of the second layer as illustrated in Figure 20 and 21.

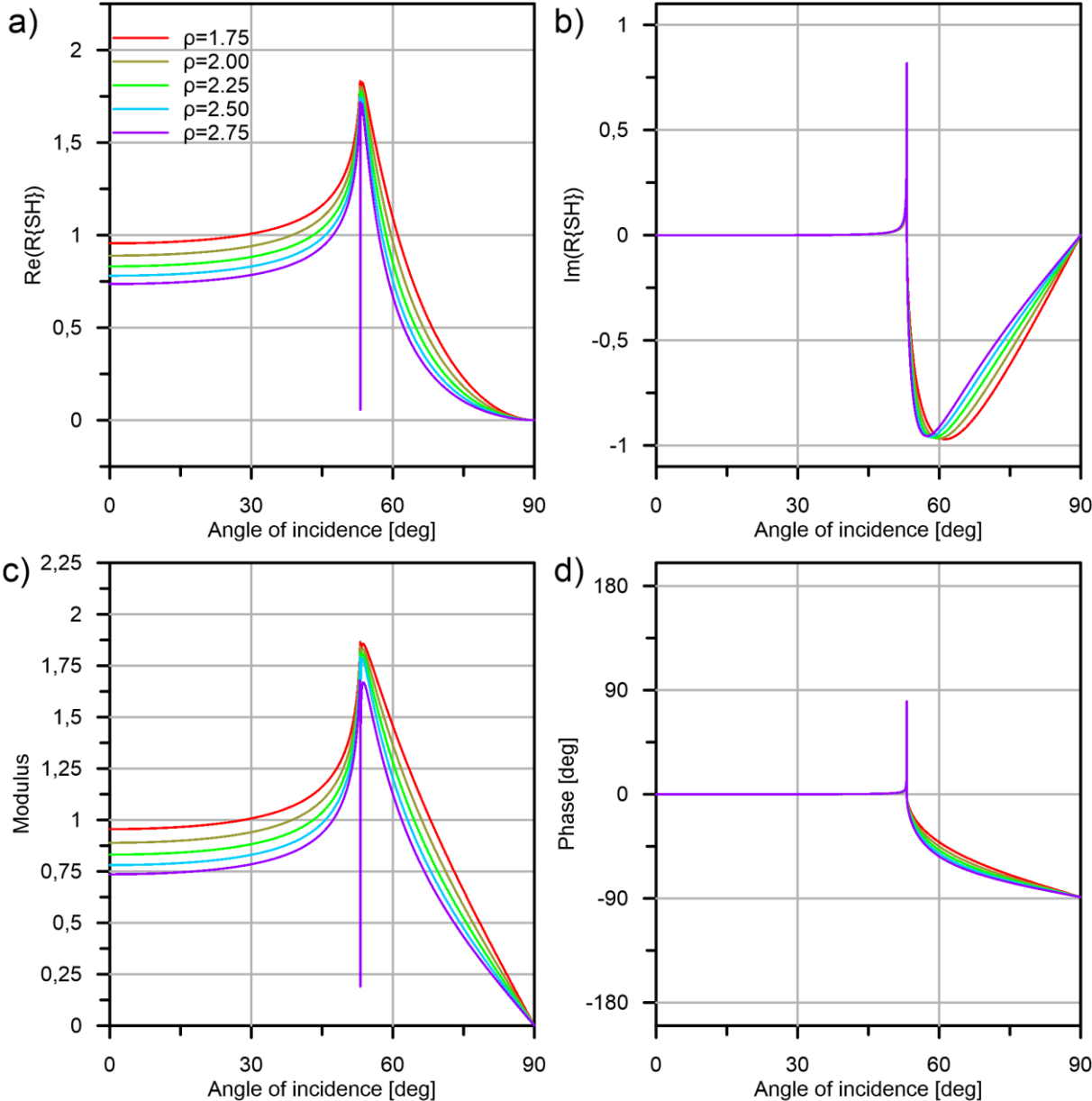


Fig. 17. a) real parts of the transmission coefficient for models with $\beta_1=2.0$ km/s, $\rho_1=2.0$ g/cm³, $Q_1=50$ and second layer characterized by $\beta_2=2.5$ km/s, $Q_2=75$ and 5 different ρ_2 values, b) imaginary parts of transmission coefficient, c) moduli of transmission coefficient, d) phases of transmission coefficient.

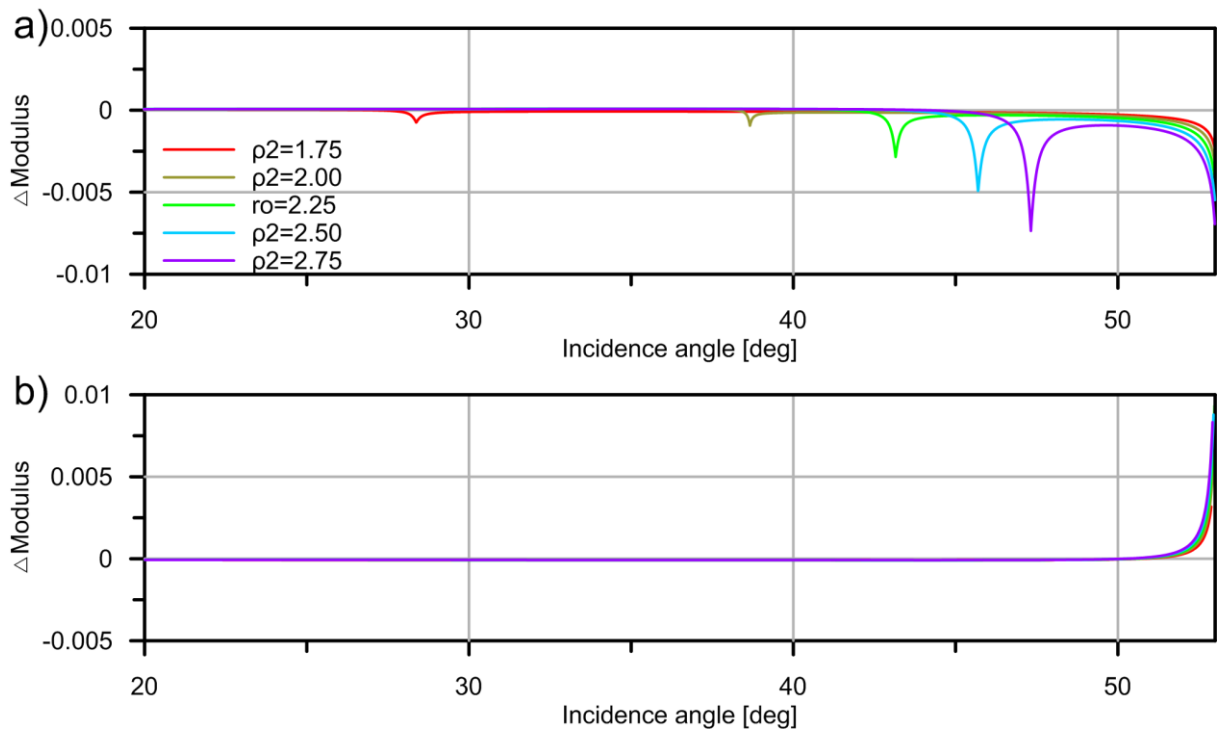


Fig. 18. a) differences between reference elastic reflection coefficients and coefficients calculated using WAC for models shown in Figure 16 – subcritical incidence, b) difference between transmission coefficients.

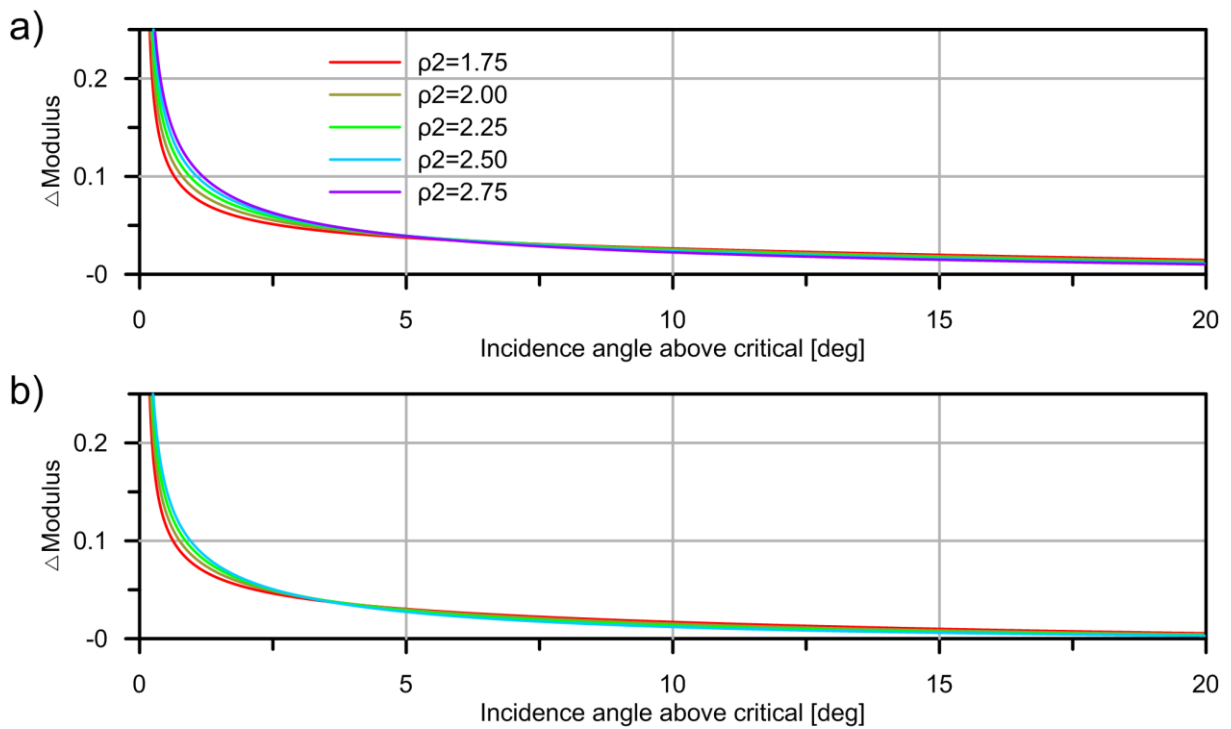


Fig. 19. a) differences between reference elastic reflection coefficient and coefficient calculated using WAC for models shown in Figure 16 – overcritical incidence, b) differences for transmission coefficient.

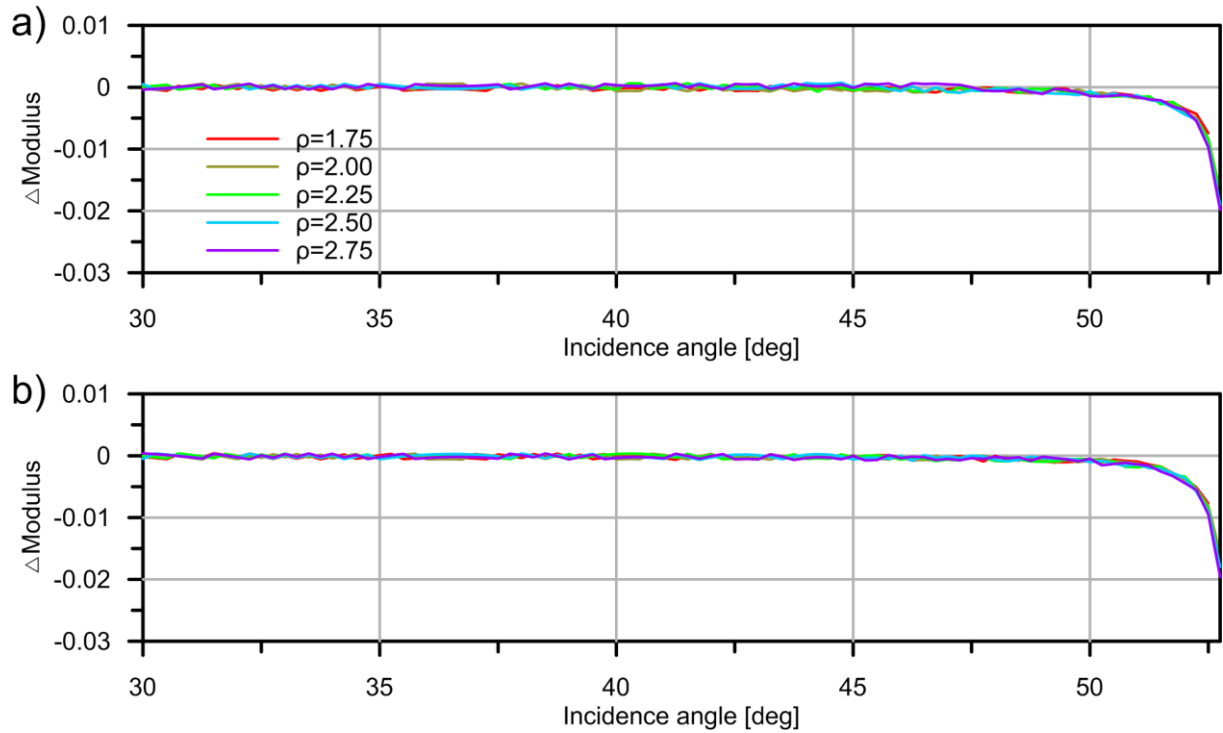


Fig. 20. a) differences between anelastic reflection coefficient calculated with exact approach of Brokešová and Červený (1998) and coefficient calculated using WAC for models shown in Figure 16 – subcritical incidence, reverberations of the curve are caused by different accuracy of computations for both methods, b) differences for transmission coefficient.

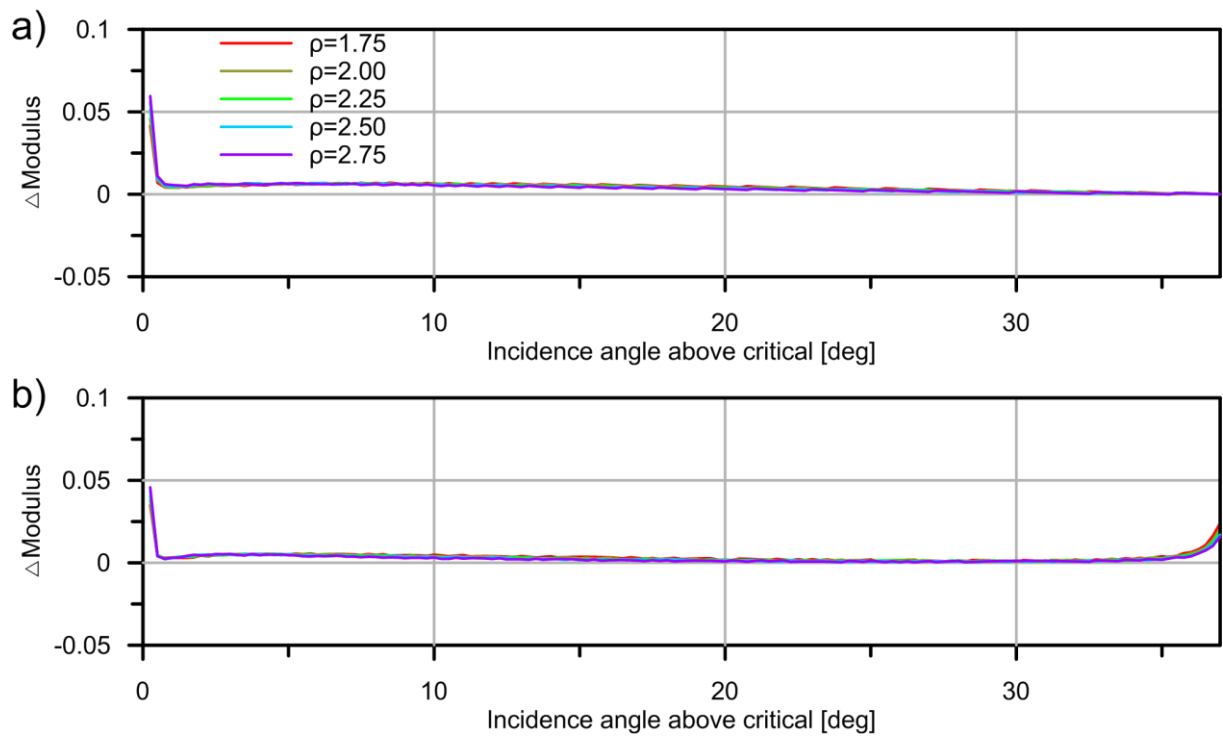


Fig. 21. a) differences between anelastic reflection coefficient calculated with exact approach of Brokešová and Červený (1998) and coefficient calculated using WAC for models shown in Figure 16 – overcritical incidence, b) differences for transmission coefficient.

The differences for the overcritical incidence are of course much higher, although they do not behave in a simple way. Just above the critical incidence, higher densities result in stronger difference in comparison to the elastic case. It is important to emphasize that it is not caused by the error of the method close to the critical angle which is stable for all investigated models. Further, for higher incident angles (in investigated case ~ 7.5 deg above the critical angle) the situation changes and it is small difference in density that results in the highest contrast to the reference elastic coefficient. Nevertheless, for those high angles, the difference in comparison to the reference is relatively small.

Besides the vicinity of the critical angle, only minor differences are present for the subcritical incidence. The strength of the modulus at the Brewster angle (Fig. 19) depends on the contrast in density between the first and the second layer, but in fact the minimum of the difference in respect to elastic reference is not at the point where $\rho_1 = \rho_2$, but below it. Figure 22 illustrate the value of the modulus of the reflection coefficient at the Brewster Angle for model with the same properties of the first and second layer as in Figure 16, but with densities of the second layer varying from 1.65 g/cm^3 (lower densities would not result in the presence of the Brewster Angle) to 3.0 g/cm^3 . We can see that the modulus of the reflection coefficient at the Brewster angle is the lowest for $\rho_2 \sim 1.85 \text{ g/cm}^3$ which is noticeably lower than the $\rho_1 = 2.0 \text{ g/cm}^3$. Note, that usually higher density implies higher value of Q . Therefore, it is not likely to encounter the model with layer that would have very low density but would be very weakly attenuative.

If we focus on the phase of calculated coefficients, differences in densities have similar effect as variations of Q – namely at the Brewster angle the change from ~ 180 (-180 degrees) to ~ 0 degree phase may be done from “positive” and “negative” side. Change of the direction is present for the density that implies minimum difference in modulus in respect to the elastic reference at the Brewster angle ($\rho_2 \sim 1.85$). Smaller the value at the Brewster angle, sharper the transition in phase.

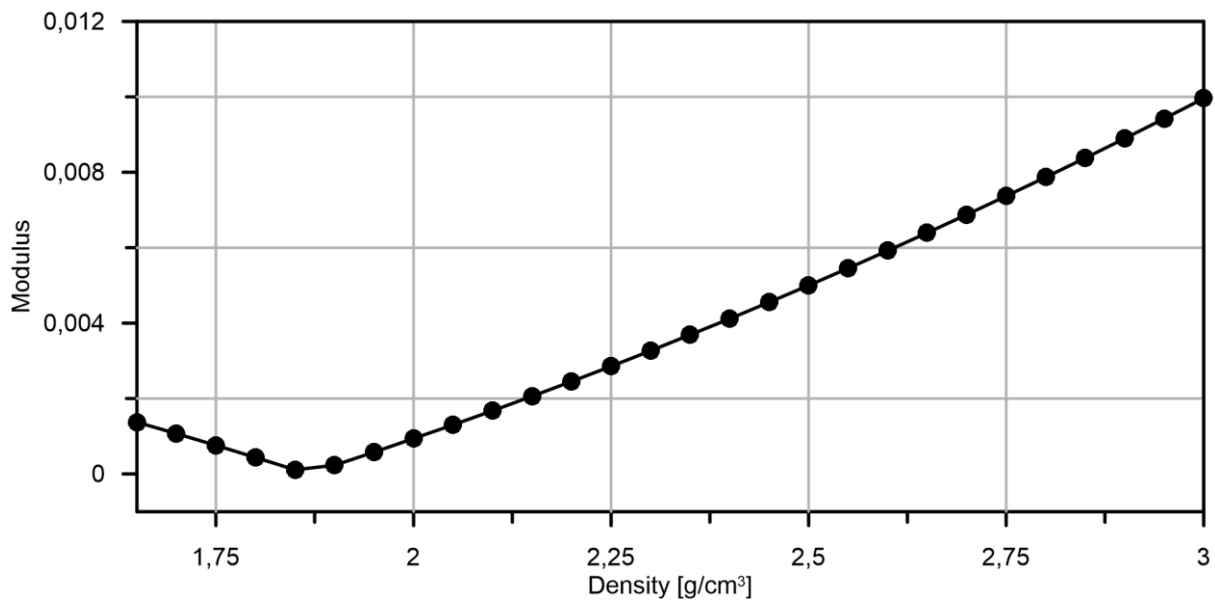


Fig. 22. Minimum value of the modulus of the reflection coefficient at the Brewster angle for models with $\beta_1 = 2.0 \text{ km/s}$, $\rho_1 = 2.0 \text{ g/cm}^3$, $Q_1 = 50$ and second layer characterized by $\beta_2 = 2.5 \text{ km/s}$, $Q_2 = 75$ and different values of the ρ_2 .

6. Reflection and Transmission coefficients for varying velocities

Variations of velocities have important influence on the shape of the R/T coefficients. It is the ratio of velocities between layers that controls presence of the critical incidence. We shall investigate the effect of changing velocity on the R/T coefficients calculated using WAC using analogous models as in the case of varying Q and ρ . Namely, the first layer is characterized by $\beta_1=2.0$ km/s, $\rho_1=2.0$ g/cm³, $Q_1=50$ and second layer is characterized by $\rho_2=2.25$, $Q_2=75$ and varying $\beta_2= 1.5, 2.0, 2.5, 3.0$ and 3.5 km/s. Figure 23 and 24 shows real, imaginary part of reflection coefficient and its modulus and phase for reflection and transmission respectively.

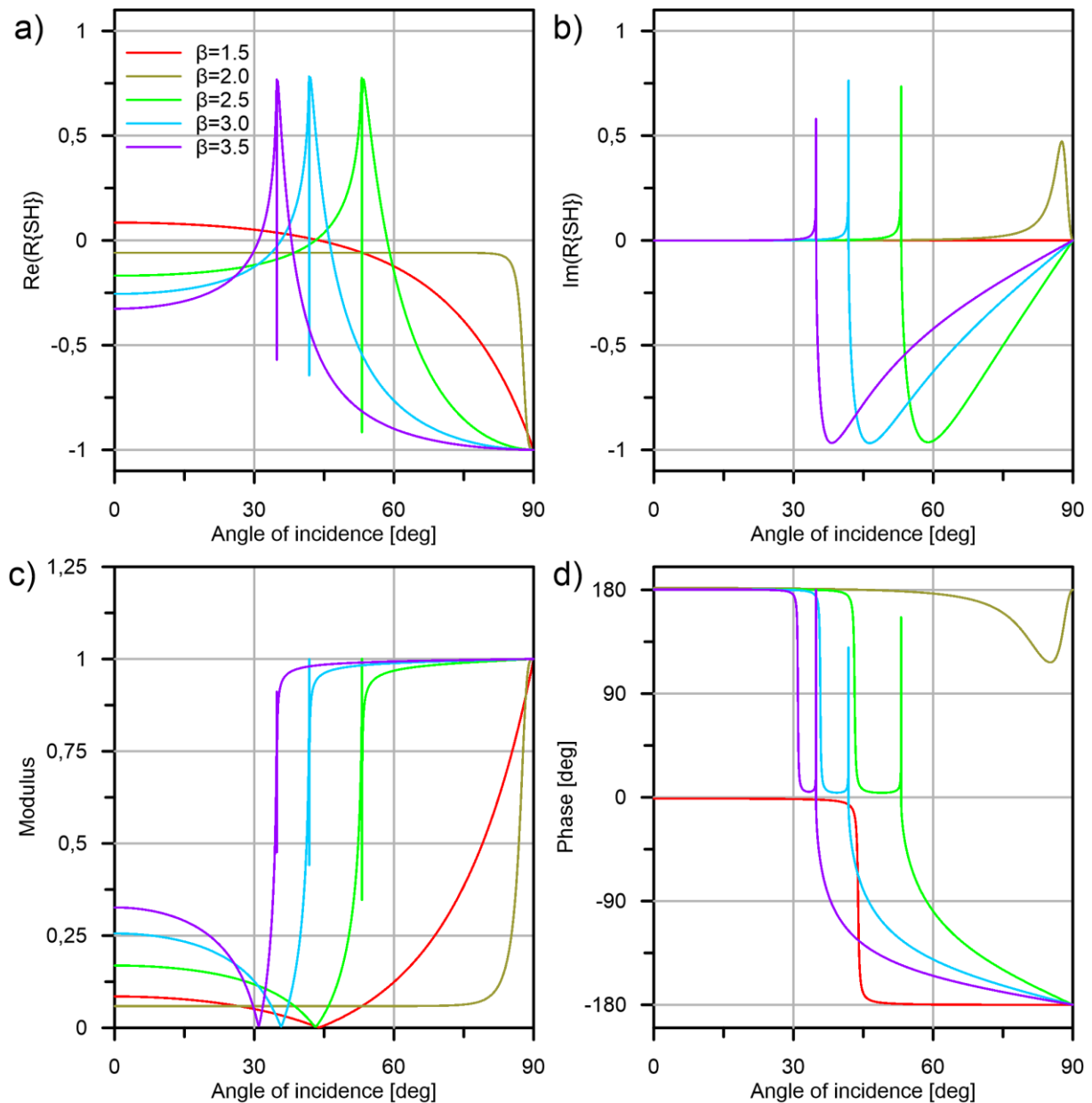


Fig. 23. a) real parts of the reflection coefficient for models with $\beta_1=2.0$ km/s, $\rho_1=2.0$ g/cm³, $Q_1=50$ and second layer characterized by $\rho_2=2.25$ g/cm³, $Q_2=75$ and 5 different β_2 values, b) imaginary parts of reflection coefficient, c) moduli of reflection coefficient, d) phases of reflection coefficient.

We can see that the variation of velocities have significant implications. For model with second layer being slower ($\beta_2=1.5$ km/s) the critical angle does not exist and therefore the effect of the attenuation on the R/T is very small for all angles. For $\beta_2 > \beta_1$, in the vicinity of the critical angle we can see the reduction of the modulus of the calculated coefficients that is analogous to the one described earlier in the study. Figures 25 and 26 show differences between anelastic and elastic moduli for sub- and over-critical incidence for investigated models. Figure 27 shows results for model where $\beta_1=\beta_2=2.0$ km/s separately as it is a special case that we shall discuss in more detail.

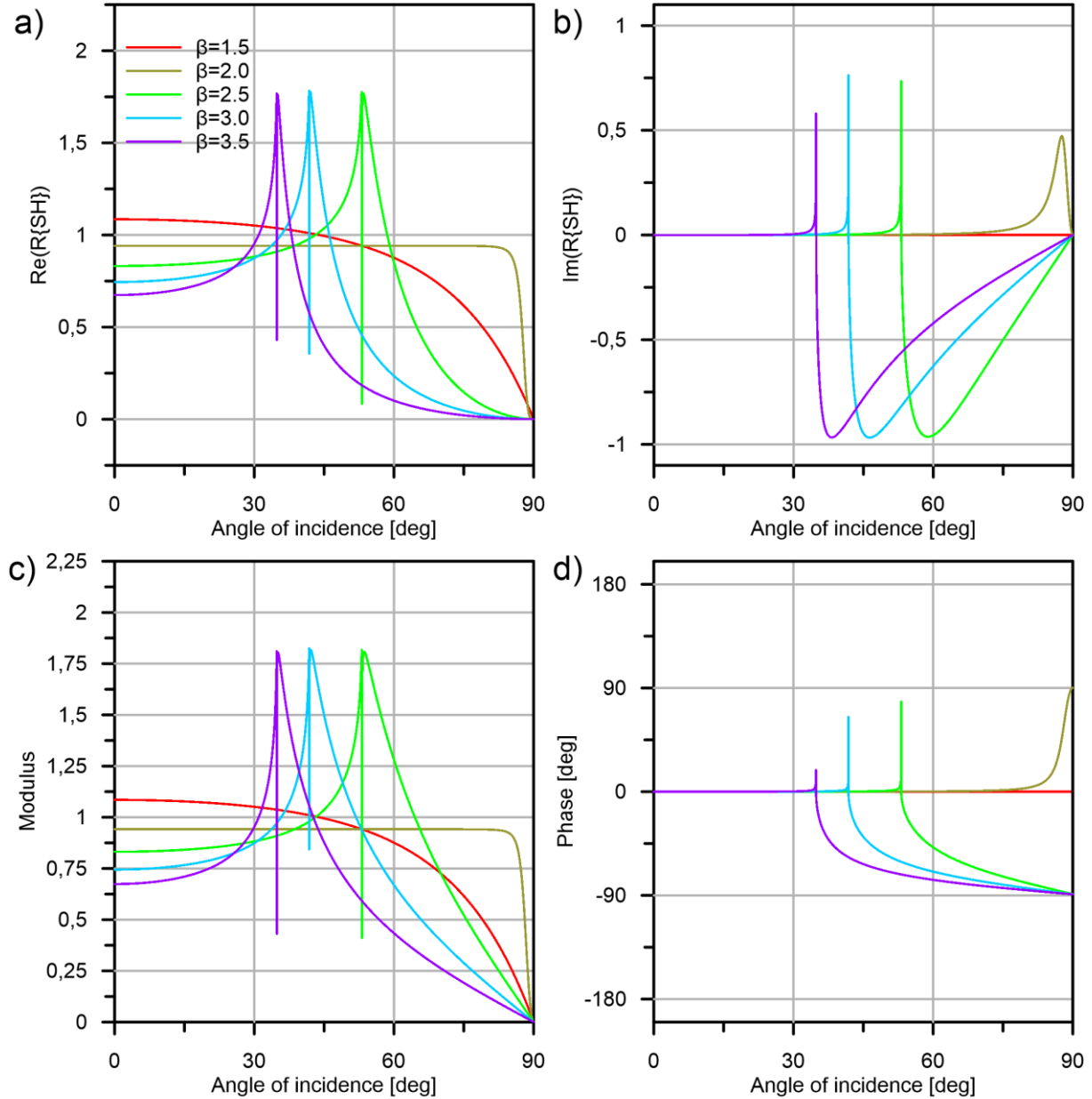


Fig. 24. a) real parts of the transmission coefficient for models with $\beta_1=2.0$ km/s, $\rho_1=2.0$ g/cm³, $Q_1=50$ and second layer characterized by $\rho_2=2.25$ g/cm³, $Q_2=75$ and 5 different β_2 values, b) imaginary parts of transmission coefficient, c) moduli of transmission coefficient, d) phases of transmission coefficient.

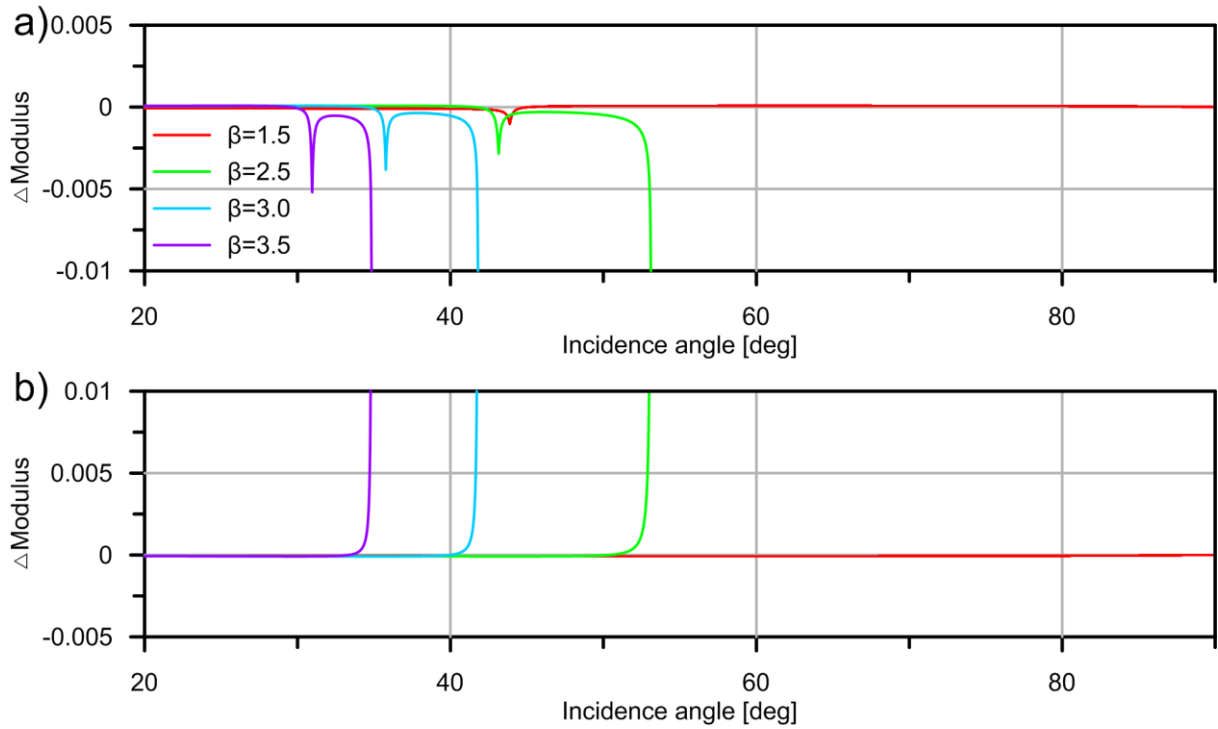


Fig. 25. a) differences between reference elastic reflection coefficient and coefficient calculated using WAC for models shown in Figure 22 – subcritical incidence, b) differences for transmission coefficient.

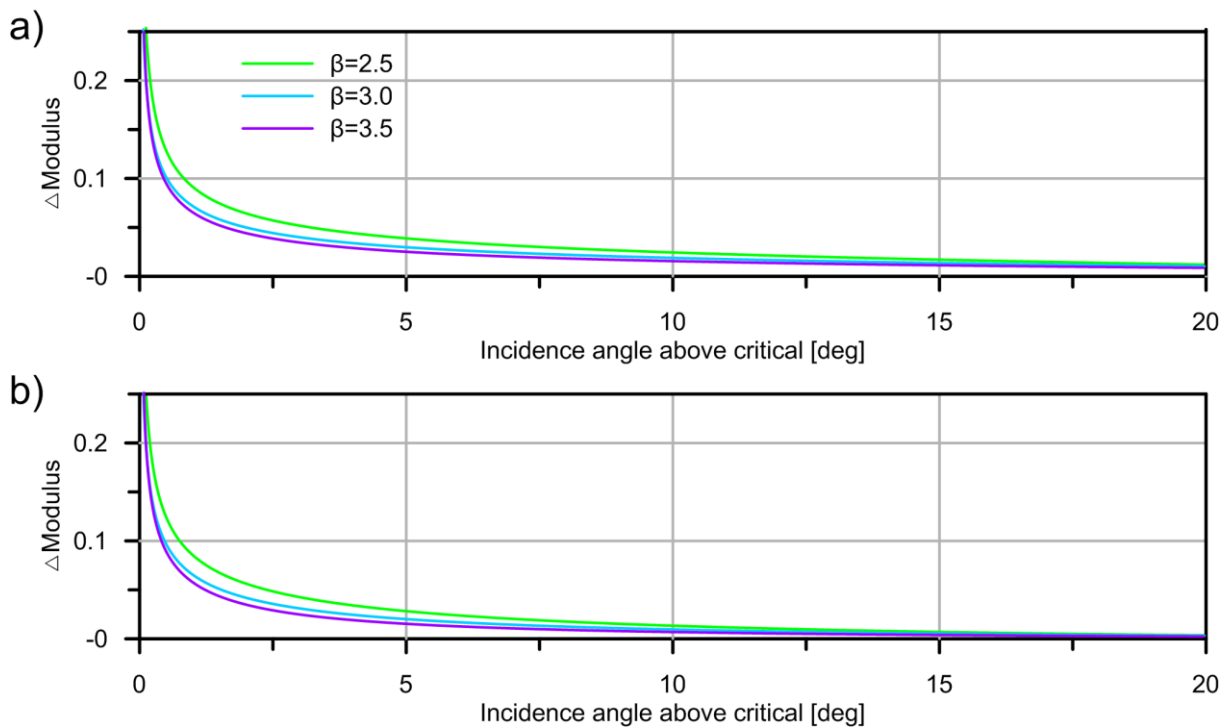


Fig. 26. a) differences between reference elastic reflection coefficient and coefficient calculated using WAC for models shown in Figure 22 – overcritical incidence, b) differences for transmission coefficient.

In the vicinity of the Brewster angle, the differences between the elastic and anelastic coefficient are greater for velocities higher in the second layer. The increased contrast in velocity for models with second fast layer results in modulus of the coefficient at the Brewster

angle being higher. If velocity of the second layer is smaller the situation is different as for small contrast there may be no Brewster angle at all. Generally for smaller velocities in the second layer the values of modulus at the Brewster angle are smaller. Interestingly for the overcritical incidence the difference between anelastic and reference elastic R/T coefficients is higher if the contrast between velocities is small. It is not caused by the errors of the perturbation approach in the vicinity of the critical angle as the intervals affected by the singularity are similar with similar values of the error.

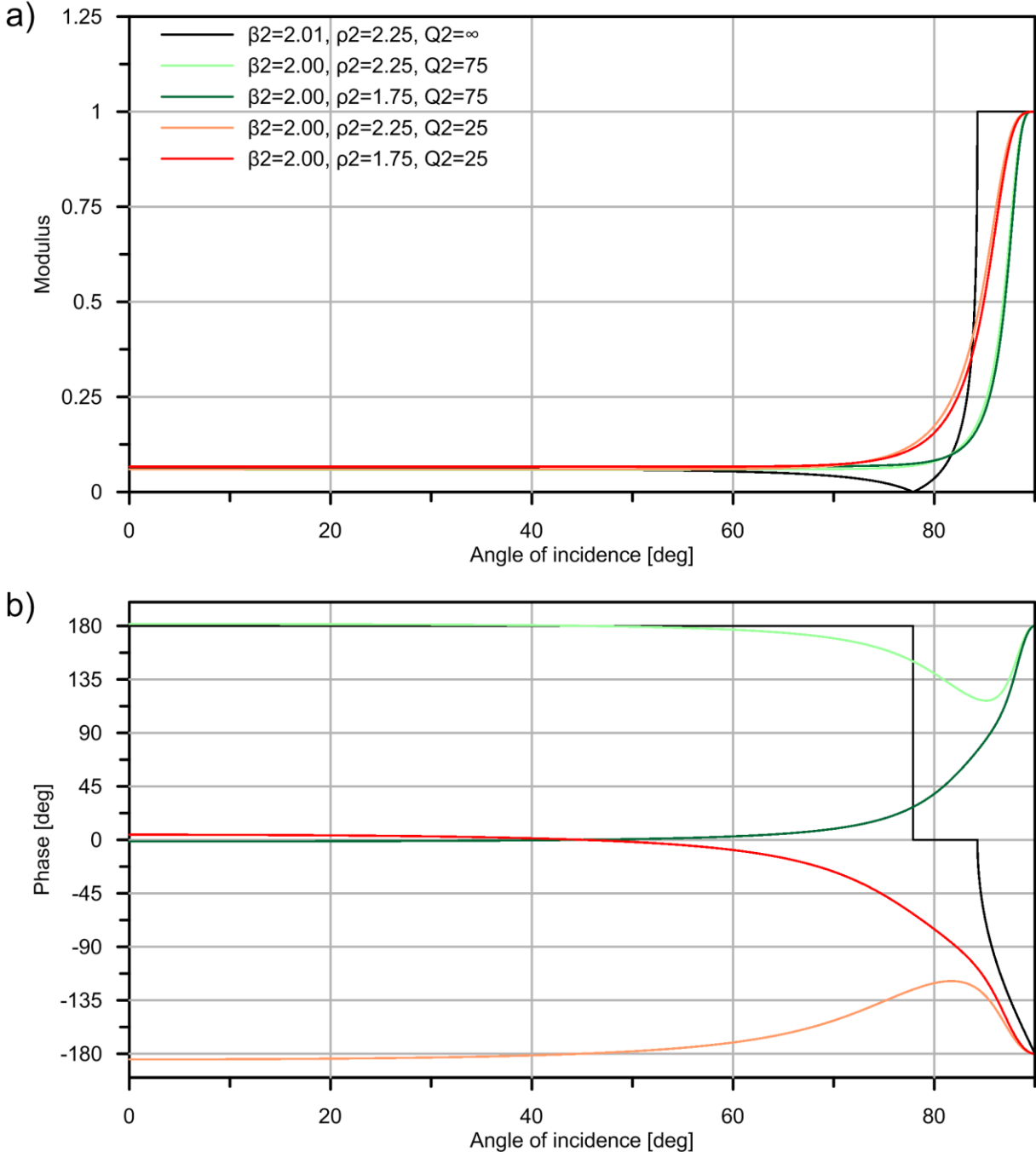


Fig. 27. a) Modulus of reflection coefficient for models with the same velocity but different values of density and attenuation - elastic case with small difference in velocity presented as a benchmark, b) phase of reflection coefficient.

In the special case where the velocities between both layers are the same, the behavior of the modulus is interesting – for broad interval of incident angles the modulus of the R/T

coefficient is constant (with a value that depends on the contrast in density between layers). Further, for incident angles close to 90 degrees the modulus of the reflection coefficient grows rapidly and approaches 1 (in case of transmission coefficient that is not shown here it decreases from ~ 1 to 0). Similar effect on modulus of the elastic reflection coefficient has presence of small difference in velocities between layers where the second one is faster. It is shown in Figure 27, where we present moduli and phases of reflection coefficient for models with the same velocity and different values of density, but we also include results for the model where both layers are elastic and second layer is characterized by $\beta_2=2.01$ km/s, $\rho_1=2.25$ g/cm³. We can see that in case of moduli presented curves for the reflection coefficient are similar. If we calculate phases of coefficient, the behavior of the curves is much more complicated and depends on relations between densities and strength of the attenuation of layers.

7. Reflection and Transmission coefficients for inhomogeneous incident waves

As we could see in the earlier part of the study the perturbation of the slowness vector of a wave is related to the strength of attenuation characterizing the medium. Nevertheless, there is a second factor that influences the attenuation vector in equations 1 and 2 – namely the inhomogeneity of the incident slowness vector (eq. 3). The quality factor of the medium is only describing the component of the attenuation vector that is parallel to the propagation vector. In the presence of inhomogeneity the attenuation vector is in fact longer than it would be implied by the Q factor itself. We can note that in the Eq. 1 and 2 it is the normal component to the interface that defines the size of the perturbation. With the presence of inhomogeneity the component of the attenuation vector normal to the interface may be enlarged or shortened. As shown by the Pšenčík and Wcisło (2018) transmitted waves are generally inhomogeneous and it may influence the calculations in case of presence of high number of layers. For models where the velocity and Q factor of the second layer is higher than in the first one, the inhomogeneity angle of the transmitted wave is higher than of the incident wave: $\gamma_1 < \gamma_t$ - note that it does not imply that $|\gamma_1| < |\gamma_t|$.

Example of the effect of inhomogeneity on the reflection and transmission coefficient is presented in Figures 28 and 29 for model with $\beta_1=2.0$ km/s, $\rho_1=2.0$ g/cm³ $Q_1=50$ and $\beta_2=2.5$ km/s, $\rho_2=2.25$ g/cm³ $Q_2=75$. The inhomogeneity of the incident wave is equal -30 and 30 degrees. The curve where the incident wave is homogeneous is included as a reference.

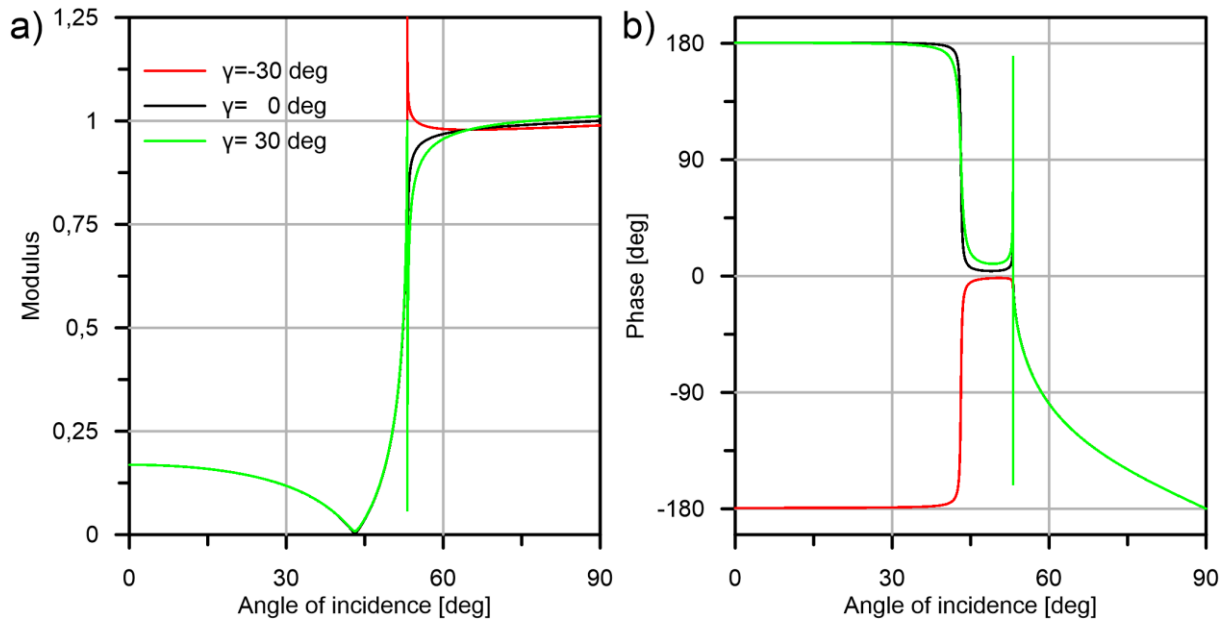


Fig. 28. a) moduli of the reflection coefficient for models with $\beta_1=2.0$ km/s, $\rho_1=2.0$ g/cm³, $Q_1=50$ and second layer characterized by $\beta_1=2.5$, $\rho_1=2.25$ g/cm³, $Q_2=75$, for inhomogeneous incident waves with $\gamma=-30$, 0 and 30 deg, b) phases of the reflection coefficient.

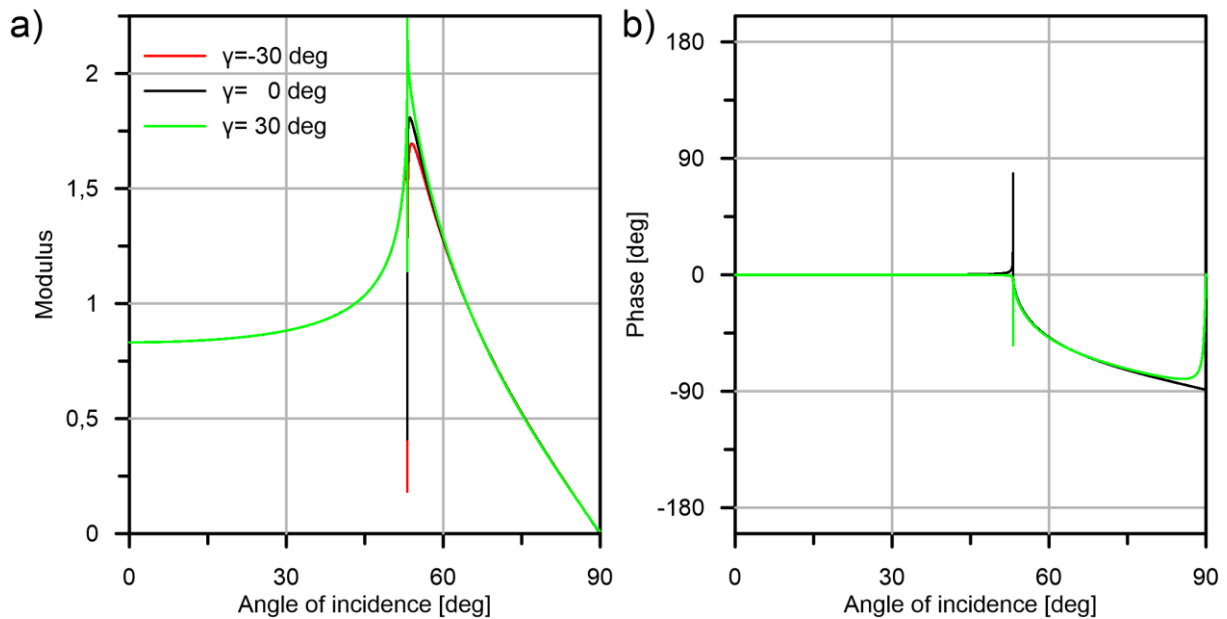


Fig. 29. a) moduli of the transmission coefficient for models with $\beta_1=2.0$ km/s, $\rho_1=2.0$ g/cm³, $Q_1=50$ and second layer characterized by $\beta_1=2.5$, $\rho_1=2.25$ g/cm³, $Q_2=75$ and for inhomogeneous incident waves with $\gamma=-30$, 0 and 30 deg, b) phases of the transmission coefficient.

Let's focus first on the interval with incidence below the vicinity of the critical angle where it is the Brewster angle that gives us biggest differences in respect to the elastic reference. The value of the modulus at the Brewster angle depends on inhomogeneity of the incident wave. For the presented model minimum of the modulus at the Brewster angle is found for the inhomogeneity of the incident wave equal ~ 18 deg. Inhomogeneity angle that corresponds to the minimum grows if the difference between velocities is small, but the difference in densities is significant. High contrast in Q between layers increases the angle where the minimum is placed as well. We illustrate it in Figure 30 where we show values of the modulus of the reflection coefficient at the Brewster angle for models with $\beta_1=2.0$ km/s,

$\rho_1=2.0 \text{ g/cm}^3$, $Q_1=50$ and second layer characterized by $\beta_2=2.5 \text{ km/s}$, $\rho_2=2.1 \text{ g/cm}^3$, $Q_2=60$, $\beta_2=2.5 \text{ km/s}$, $\rho_2=2.25 \text{ g/cm}^3$, $Q_2=75$ and $\beta_2=2.1 \text{ km/s}$, $\rho_2=2.5 \text{ g/cm}^3$, $Q_2=100$ respectively. Inhomogeneity angle that corresponds to the minimum value of the modulus at Brewster angle for given model delineates different direction of the approach of the phase of reflection coefficient from $\sim\pm 180$ degrees to ~ 0 degrees.

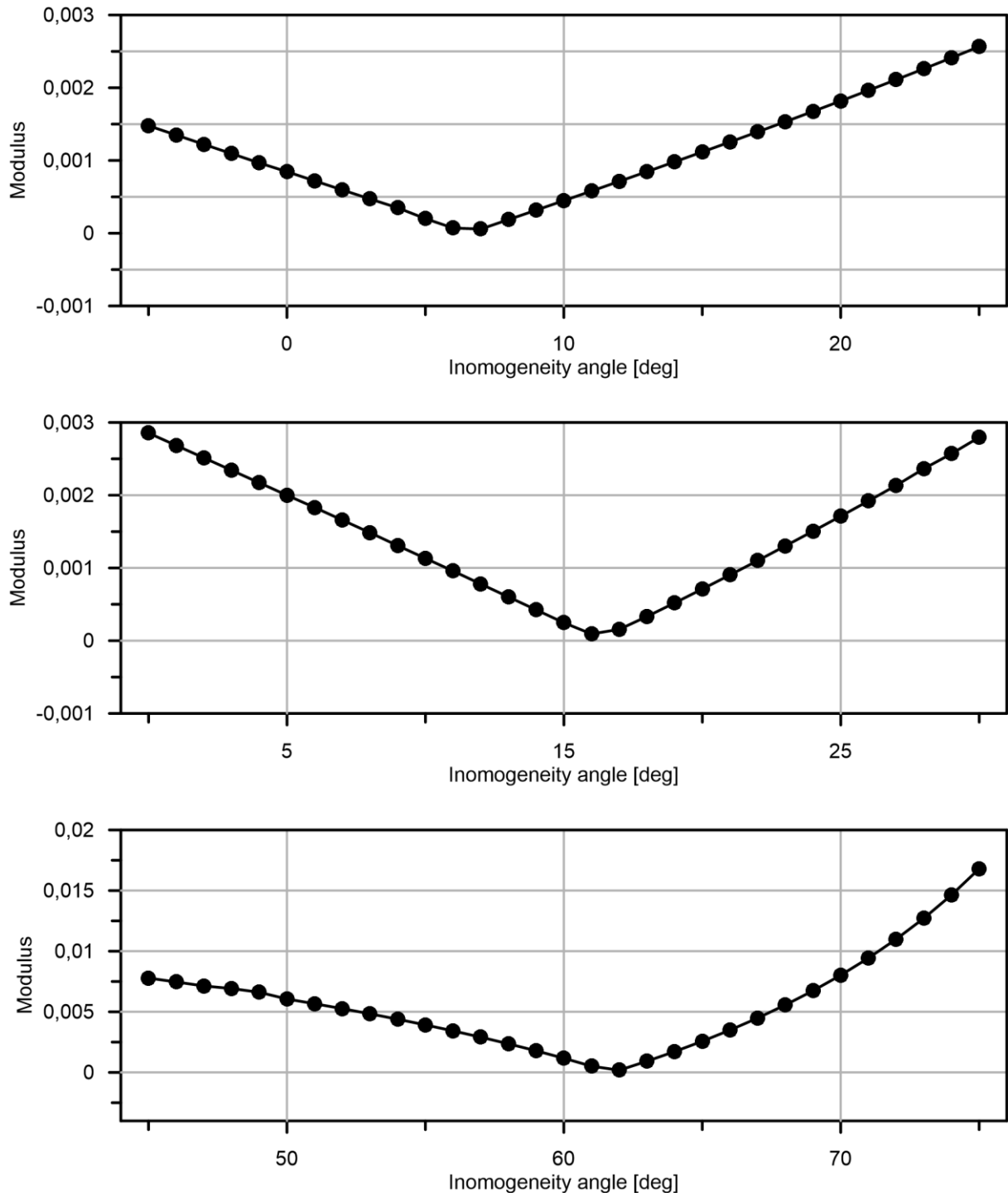


Fig. 30. Minimum value of the modulus of the reflection coefficient at the Brewster angle for models with $\beta_1=2.0 \text{ km/s}$, $\rho_1=2.0 \text{ g/cm}^3$, $Q_1=50$ and second layer characterized by $\beta_2=2.5 \text{ km/s}$, $\rho_2=2.1 \text{ g/cm}^3$, $Q_2=60$ (top panel), $\beta_2=2.5 \text{ km/s}$, $\rho_2=2.25 \text{ g/cm}^3$, $Q_2=75$ (middle panel) and $\beta_2=2.1 \text{ km/s}$, $\rho_2=2.5 \text{ g/cm}^3$, $Q_2=100$ (bottom panel) and different inhomogeneity angle of the incident wave.

When discussing effects of inhomogeneity of the wave for the interval starting from the vicinity of the critical angle up to 90 degree incidence we shall be more cautious. For certain angles of incidence values of modulus of reflection coefficient are incorrect (>1). In case of models used in Figure 28, for the one with inhomogeneity $\gamma_1 = -30$ degrees we have a clear spike above the critical angle (similar spike is present for the transmission coefficient) - this is similar to the case of medium where $\beta_1 < \beta_2$ but $Q_1 > Q_2$ that was shown in Figure 10. As shown in Figures 28 and 29 for inhomogeneity angle $\gamma_1 = 30$ degrees the discrepancy is present as well but it is for the interval where angles are close to horizontal incidence that the reflection coefficients slightly exceeds 1. To assess the size of errors for inhomogeneous incident waves we calculate differences between elastic coefficients and coefficients calculated using WAC (Figure 31) and differences between WAC and results obtained using exact approach of Brokešová and Červený (Figure 32). We show results with media properties the same as in Figure 28 but with γ_1 equal -15, -5, 5, 15, 25, and 35. In those figures we show values for incident angles above 45 deg which include critical incidence.

Figures 31 and 32 show that for certain models, significant part of differences in respect to elastic reference is caused by inaccuracy of WAC. The Failure of the method that is present for 2-3 deg before critical incidence is caused by singularity and has consistent character for both positive and negative inhomogeneity. For overcritical incidence the character of the discrepancy is more complicated. In case of reflection coefficient we can distinguish 3 types of the behavior of the discrepancy that depends on the inhomogeneity of the incident wave. For negative inhomogeneity of the incident wave, the error steadily changes downwards. For small negative inhomogeneity the error may be at the beginning positive (underestimation of the modulus), then further it decreases its value (we do not consider here the absolute value of the error). If the negative inhomogeneity is stronger the error of the WAC is negative (overestimation of the modulus) almost instantly after the critical angle, and then further decreases. Secondly, for small positive inhomogeneity, the error of the WAC is always positive and it also decreases with increasing angle of incidence but do not cross 0 to negative values. Third type - for higher positive inhomogeneity (in case of presented model it is for $\gamma_1 \sim 18$ deg) values of the modulus for the angles just after the critical are strongly overestimated, but with increasing incidence the error switches side, and further its absolute value decreases. The positive inhomogeneity angle of the incident wave that delineates the last type of behavior depends on the model and behaves similarly to the inhomogeneity angle that determines minimum of the modulus at the Brewster angle. At last, for incidence angles $\sim 88-90$ degrees the error of the WAC may change rapidly – as visible in the Figure 32.

In case of transmission coefficients the error of the WAC behaves in a similar way as in the case of the reflection coefficient. Nevertheless its absolute value is generally smaller. The most problematic case is for strong positive inhomogeneity of the incident wave. Additionally, again for very high incidence angles ($\sim 88-90$ deg) there is a presence of significant error in calculated phases (as result phase in Figure 29 shift to 0 degree for incidence close to the horizontal).

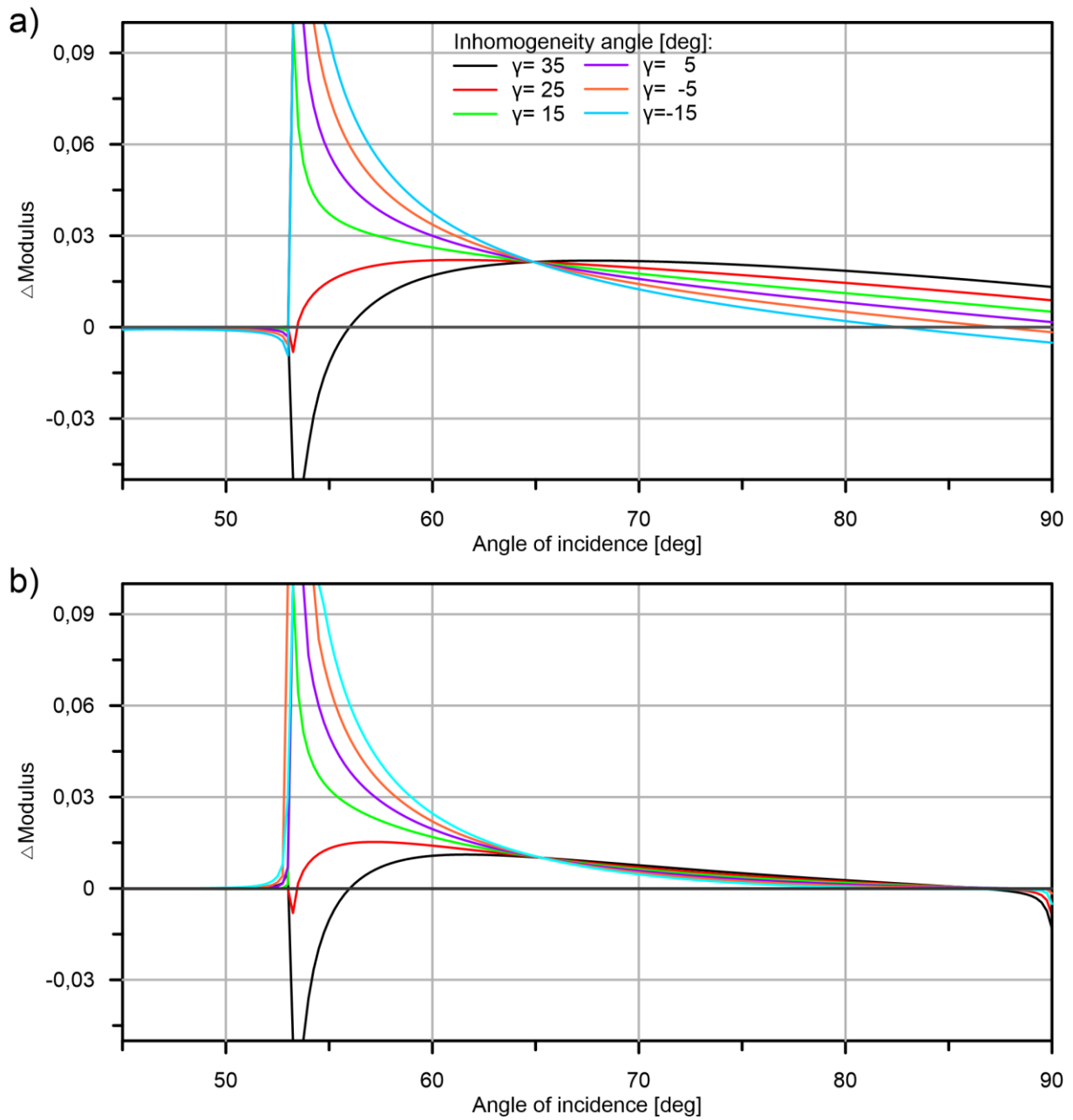


Fig. 31. a) differences between reference elastic reflection coefficients and coefficients calculated using WAC for models with $\beta_1=2.0$ km/s, $\rho_1=2.0$ g/cm³, $Q_1=50$ and second layer characterized by $\beta_2=2.5$ km/s, $\rho_2=2.25$ g/cm³, $Q_2=75$ for various values of inhomogeneity of the incident wave, b) differences calculated for transmission coefficients.

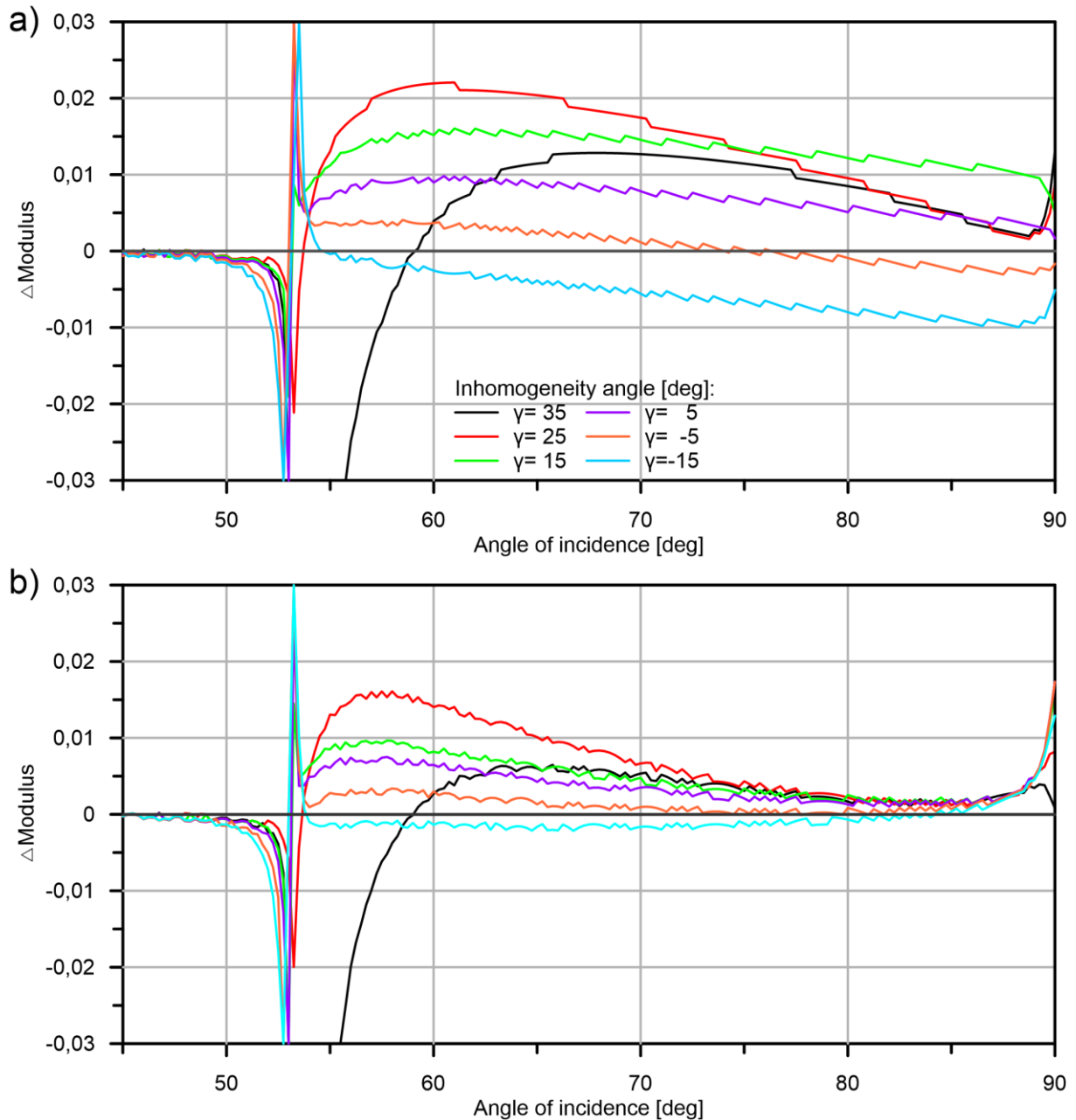


Fig. 32. a) differences between anelastic reflection coefficient calculated with exact approach of Brokešová and Červený (1998) and coefficient calculated using WAC for models shown in Figure 30, reverberations of the curves are caused by different accuracy of computations for both methods, b) differences for transmission coefficients.

8. Inaccuracy for models with faster, but more attenuative second layer

In Figure 10 we could see that for models with faster, but more attenuative second layer the method fails above the critical angle much more abruptly than for other models. The values obtained using WAC in case of reflection for certain interval are above 1 and the range of the angles where the method fails is much broader than in other cases where usually it is ± 2 degrees. To investigate the limits of the approach for this unusual case we have calculated the R/T coefficients for models with first layer with $\beta_1=2.0$ km/s, $\rho_1=2.0$ g/cm³ $Q_1=50$ and second layer characterized by $\beta_2=2.5$ km/s, $\rho_2=2.25$ g/cm³, and $Q_2 < Q_1$ with increasing difference

between layers. Obtained results were compared with direct approach of Brokešová and Červený. Figure 32 shows how fast the WAC approximation converges to the direct results - specifically in how extensive interval the difference between the calculated coefficients is above 0.01. We can see that in principle higher contrast in Q values results in the interval that has inaccurate results being broader. It is worth to note that the inaccuracy is smaller if we consider transmission coefficients. Naturally, as it was shown in earlier parts of the study, calculated coefficients depend not only on the Q factors describing the media but, on the density of the rock and SH- wave velocities as well. As it was shown, increasing contrast in seismic velocities reduce the differences between coefficients calculated using WAC and its elastic reference for the overcritical incidence. High contrast in velocities in fact reduces the extent of the interval that provides inaccurate results. To illustrate this particular effect, Figure 33 includes results for the analogous model to the one described before, but with $\beta_2=3.0$ km/s. We can clearly see that the interval with inaccurate values of the calculated coefficient is lower for models with higher contrast in velocities and it is especially visible if the Q_2 is significantly lower than Q_1 .

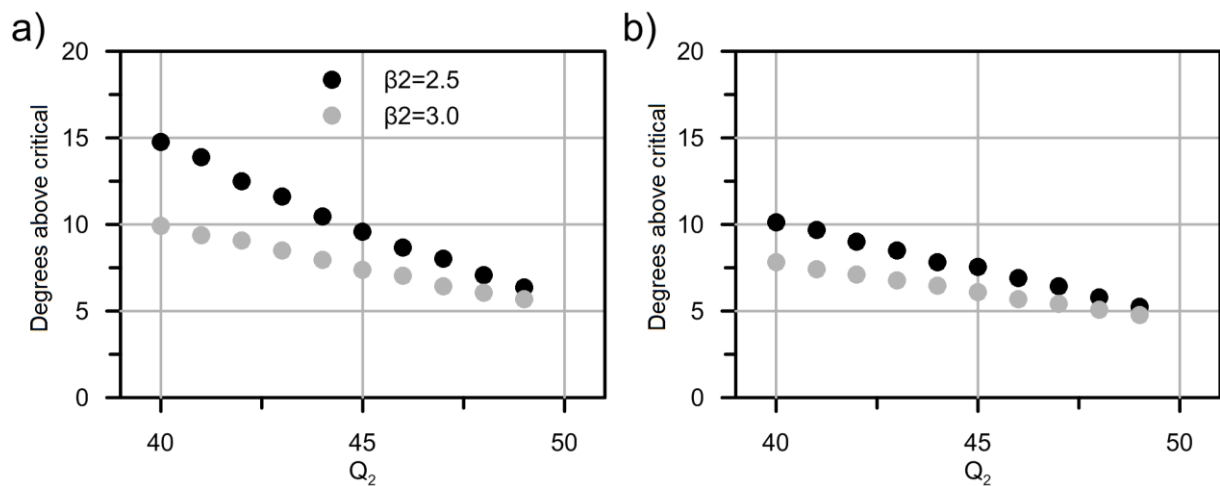


Fig. 33 a) length of the interval (in degrees) where the WAC provides results of the reflection coefficient with the difference to exact approach of Brokešová and Červený (1998) above 0.01 for models with $\beta_1=2.0$ km/s, $\rho_1=2.0$ g/cm³ $Q_1=50$ and second layer characterized by $\beta_2=2.5$ (3.0) km/s, $\rho_2=2.25$ g/cm³ and different values of Q_2 smaller than Q_1 b) length of the interval for transmission coefficient.

9. Conclusions

We investigated effects of attenuation on reflection and transmission coefficients using Weak Attenuation Concept. Generally presence of attenuation implies very small differences in respect to the elastic reference for subcritical incidence. The interval where the effect is the strongest is in the vicinity of the Brewster Angle where in contrast to the elastic case the modulus of the reflection coefficient is non zero (although in most cases we should not expect that it should be greater than 0.01-0.02). Attenuation visibly influences the reflection and transmission coefficients in the vicinity of the critical angle of incidence. WAC fails in the vicinity of the critical angle but generally in case of incident wave that is homogeneous, the interval that is significantly influenced by the singularity is within ± 2 degrees of the critical angle for most of the models. Therefore, we can use the perturbation approach to investigate the behavior of the reflection and transmission coefficient in the broader vicinity of the

critical angle. Generally the modulus of the coefficients in anelastic media from the vicinity of the critical angle onward is smaller than in the elastic case, which indicates dispersion of the energy at the boundary. Difference in respect to the elastic reference for overcritical incidence grows if the contrasts in quality factor and density between layers increase. In opposite, for the overcritical incidence, if the contrast between the S wave velocity grows, the difference in respect to the elastic modulus is smaller. Inhomogeneity of the incident wave does not influence strongly reflection and transmission coefficients in the subcritical region, although for overcritical incidence it reduces the accuracy of the approximation. If the inhomogeneity of the incident wave is strong, the inaccuracy of the WAC may be of the same order as the difference with respect to elastic reference for the overcritical incidence. In such a case the use of the WAC is not advised.

Acknowledgments

The research has been supported by the Grant Agency of the Czech Republic under contract 16-05237S, by the Ministry of Education, Youth and Sports of the Czech Republic within research project CzechGeo/EPOS LM2015079, and by the members of the consortium “Seismic Waves in Complex 3-D Structures” (see “<http://sw3d.cz>”).

References

- Aki, K. and Richards, P.G., 2002. *Quantitative Seismology*, 2nd ed., University Science Books.
- Barton, N., 2006, *Rock Quality, Seismic Velocity, Attenuation and Anisotropy*, 1rd ed., CRC Press.
- Brokešová, J. and Červený, V., 1998. Inhomogeneous plane waves in dissipative, isotropic and anisotropic media. Reflection/transmission coefficients. *Seismic waves in complex 3-D structures*, **7**, 57-146, Available at: <http://sw3d.cz>.
- Buchen, P.W., 1971. Reflection, transmission and diffraction of SH-waves in linear viscoelastic solids. *Geophys. J.R. astr. Soc.*, **25**, 97-113.
- Daley, P.F. and Krebes, E.S., 2015. Anelastic (poroviscoelastic medium – the S_H -wave problem. *J. Seism. Explor.*, **24**, 103-120.
- Gajewski D. and Pšenčík I., 1992. Vector wavefields for weakly attenuating anisotropic media by the ray method. *Geophysics*, **57**, 27-38.
- Helle, H.B., Pham, N.H. and Carcione J.M., 2003, Velocity and attenuation in partially saturated rocks: poroelastic numerical experiments. *Geophys. Pros.*, **51**, 551-566.
- Pšenčík, I. and Wcisło, M., 2018. SH-wave reflection/transmission coefficients in isotropic, weakly attenuating media. *Seismic waves in complex 3-D structures*, **28**, 113-134, Available at: <http://sw3d.cz>.
- Ursin, B., Carcione, J.M. and Gei, D., 2017. A physical solution for plane SH waves in anelastic media. *Geophys. J. Int.*, **209**, 661-671.